12

Zero-Mass Approach to Counterterms

Massive Feynman integrals containing more than one loop momentum are hard to evaluate. Fortunately, the understanding of the critical behavior of the field theory requires only knowledge of the divergent counterterms. In the last chapter we have seen that their calculation reduces to the calculation of logarithmically divergent diagrams without tadpole parts for Z_g and Z_{m^2} and of quadratically divergent diagrams without tadpole parts for Z_ϕ. From the superficial divergence of the latter. only the mass-independent part is needed. In addition, the superficial divergences of the logarithmically divergent diagrams are independent of the mass and of the external momenta. These properties have the important consequence that masses and external momenta of Feynman integrals may be modified in a variety of ways without changing the counterterms. In particular, masses and external momenta may be set equal to zero as long as this does not produce unphysical IR-divergences. We shall see that overall IR-divergences do not occur if at least one external momentum is kept nonzero. There are different ways of choosing the nonzero momentum, and the corresponding mathematical modifications of Feynman integrals are called *infrared rearrangement* (IRR) [1]. A suitable rearrangement allows us to simplify considerably the calculation of counterterms in a massive theory.

In many Feynman integrals, the single nonzero external momentum is still an obstacle to an analytical calculation. In this case one employs a more drastic IR-rearrangement by admitting a final nonzero external momentum which *does* generate unphysical *IR-divergences*. These must be properly identified and subtracted to arrive at the desired UV-counterterms.

The minimal subtraction scheme which is so convenient for regularizing the theory has, unfortunately, an unpleasant feature as far as the new unphysical IR-divergences are concerned. The new divergences have the same $1/\varepsilon^i$ -pole form as the UV-divergences. The identification and subtraction of the infrared parts in the total counterterms are therefore nontrivial. These parts will be called *IR-counterterms*, for brevity, and we shall develop a diagrammatic method for calculating them for each Feynman diagram. We shall construct so-called *IR-diagrams* which must, of course, be such that no new UV-divergences arise. This procedure leads, unfortunately, to a proliferation of diagrams, but these have the advantage of containing only massless lines, which greatly simplifies the associated Feynman integrals. In some cases, this is the only way to find an analytic result for the UV-counterterms.

In this chapter we describe a recursive diagrammatic construction and subtraction of IR-divergences which proceeds by close analogy with the subtraction of UV-subdivergences. The combined recursive scheme will eventually be formulated as an extension of the R-operation, called R^*-operation [2, 3].

As a basis for understanding the IR-divergences of Feynman integrals, in which one or more masses and external momenta are set equal to zero, we introduce the technique of *infrared power counting*. This will help us decide which masses and external momenta can be set equal

to zero without changing the counterterms. Subsequently, IR-rearrangement will be explained, and the ensuing additional IR-divergences will be removed.

12.1 Infrared Power Counting

Masses and external momenta ensure the infrared finiteness of all Feynman integrals. If these dimensional parameters are all set equal to zero, IR-divergences will appear. In dimensional regularization, they manifest themselves as pole terms $1/\varepsilon^i$, making them indistinguishable from UV-divergences. To understand the relation between the two types of divergences, we must study the properties of Feynman integrals in the small-momentum regime.

For this purpose, let us rescale all loop momenta in a Feynman integral I_G by a factor σ, and suppose that the integral behaves for $\sigma \to 0$ like

$$I_G \propto \sigma^{-\tilde{\omega}} \qquad \text{for } \sigma \to 0. \tag{12.1}$$

The number $\tilde{\omega}(G)$ is called the *superficial degree of IR-divergence*. An integral is divergent in the infrared if $\tilde{\omega}(G) \geq 0$. Any line containing a mass or an external momentum does not contribute to the superficial IR-divergence. It does, however, reduce the degree of UV-divergence $\omega(G)$. This implies

$$\omega(G) \neq -\tilde{\omega}(G). \tag{12.2}$$

In a massless theory, an external momentum supplies a Feynman integral with an *IR-cutoff* which removes its superficial IR-divergence. This does not yet imply that the entire Feynman integral is IR-convergent. For this to happen, the massless diagrams in four dimensions have to possess *nonexceptional* external momenta. Only then can we rule out IR-subdivergences. Recall that according to the definition on page 140, external momenta are nonexceptional if none of their partial sums vanishes. In a ϕ^4-theory, the external momenta of two- and four-point diagrams are nonexceptional as long as they do not vanish. For this reason, we can always calculate all counterterms from massless diagrams.

If the external momenta of a diagram are exceptional, a subdiagram can be separated from the remaining diagram by cutting lines which do not carry external momenta. Such a subdiagram produces an IR-divergence in the Feynman integral. As an example of an infrared divergence arising in this way, take the Feynman integral

$$\sim \int \frac{d^4p}{(2\pi)^4} \frac{1}{\mathbf{p}^4(\mathbf{p}-\mathbf{k})^2} = \int \frac{d^4p}{(2\pi)^4} \frac{1}{(\mathbf{p}-\mathbf{k})^4\mathbf{p}^2}\,. \tag{12.3}$$

The ϕ^2-insertion on the upper line may be considered as a ϕ^4-vertex with two amputated lines of zero external momentum. The momenta are therefore exceptional. The flow of the remaining external momentum can then be chosen as specified in the first integral in (12.3), where it enters and leaves through one of the external lines on the right and left. The integral in (12.3) diverges logarithmically in the infrared, with $\tilde{\omega}(G) = 0$. Note that the original character of the vertex at the top is irrelevant to this divergence, which also would have arisen if the top vertex had been a three-point, five-point, or higher vertex.

In general, the degree of IR-divergence for a massless diagram G is found as follows. One constructs from G a subdiagram $\tilde{\gamma}$ by shrinking all lines which do not contribute to the IR-divergence. These lines are identified by searching for the maximal set of propagators which become singular at different points in momentum space. The shrinking produces a new vertex referred to as *virtual vertex*. In the diagram in (12.3), we may either shrink the upper line or the lower line because the external momenta flowing through them do not contribute to the

same IR-divergence. In fact, only the integration over the upper lines with the ϕ^2-vertex is IR-divergent. The subdiagram $\tilde{\gamma}$ is found either by shrinking all lines to a new vertex which carry an external momentum, or by shrinking all lines which do not. In some cases, several subdiagrams $\tilde{\gamma}$ have to be formed and analyzed to find all IR-counterterms. But we shall not need more than one nonzero external momentum. For this reason, the connectedness of the diagram will always lead to a shrunk diagram with only a single virtual vertex.

For the diagram (12.3), the shrunk subdiagram is $\tilde{\gamma} =$, omitting the irrelevant external lines.

An arbitrary shrunk diagram satisfies the following topological equations:

$$L(\tilde{\gamma}) = I(\tilde{\gamma}) - [V(\tilde{\gamma}) + 1] + 1\,, \tag{12.4}$$

$$2I(\tilde{\gamma}) = 4V(\tilde{\gamma}) + n\,, \tag{12.5}$$

where $L(\tilde{\gamma})$, $I(\tilde{\gamma})$, and $V(\tilde{\gamma})$ are the numbers of loops, internal lines, and vertices of the shrunk diagram. The number $V(\tilde{\gamma})$ does not include the virtual vertex arising from the shrinking. The number n counts the number of lines emerging from this vertex. The degree of IR-divergence of G is now given by the negative degree of UV-divergence of the shrunk diagram $\tilde{\gamma}$, which is

$$\omega(\tilde{\gamma}) = L(\tilde{\gamma})D - 2I(\tilde{\gamma}). \tag{12.6}$$

Thus, a diagram G is IR-divergent if the degree of UV-divergence of $\tilde{\gamma}$ is $\omega(\tilde{\gamma}) \leq 0$. Inserting relations (12.4) and (12.5) for the shrunk diagram, we obtain an equation for the superficial degree of IR-divergence:

$$\tilde{\omega}(G) = -\omega(\tilde{\gamma}) = -L(\tilde{\gamma})D + 2I(\tilde{\gamma}) = L(\tilde{\gamma})(4 - D) - n. \tag{12.7}$$

For 1PI diagrams G, the number n is never smaller than two, such that IR-convergence is guaranteed for $D = 4$. The mass can thus be set equal to zero without generating IR-divergences as long as the external momenta are nonexceptional. This means that we can perform all calculations with massless integrals. This result holds also for 1PI subdiagrams, thus eliminating possible IR-subdivergences. In 1PI subdiagrams, the IR-regulating role of external momenta is played by the loop momenta of the remaining diagram flowing into the subdiagram.

The IR-situation in our calculations is less trivial because these are performed in $D = 4 - \varepsilon$ dimensions. Then, according to Eq. (12.6), the degree of divergence depends on the number of loops $L(\tilde{\gamma})$, and therefore on the order of perturbation theory:

$$\tilde{\omega}(G) = -\omega(\tilde{\gamma}) = L(\tilde{\gamma})\varepsilon - n\,. \tag{12.8}$$

This gives rise to a small-momentum power behavior $|\mathbf{k}^2|^{n - L(\tilde{\gamma})\varepsilon}$ of the counterterms of the vertex functions. Such a power behavior is of the type discussed earlier in Eq. (9.74), and becomes compatible with the necessary locality of the counterterms only after an expansion in powers of ε.

12.2 Infrared Rearrangement

In the last section we have seen that in 1PI two- and four-point ϕ^4-diagrams with nonzero external momenta, the masses can be set equal to zero without generating IR-divergences. Thus, the four-point diagrams contributing to Z_g and Z_{m^2}, and the two-point diagrams contributing to Z_ϕ can be calculated with zero mass. We also know from Sections 11.7 and 11.8 that the renormalization constants can be calculated from diagrams whose divergence is only logarithmic,

if the differentiations are applied directly to the integrands. Since the pole terms of logarithmically divergent diagrams are independent of the external momenta, we may wonder whether the external momentum could not be set to zero as well, thus simplifying the calculations further. Unfortunately, this is not possible. If we were to do this, all lines of an integral would contribute to the IR-behavior, implying that the superficial degree of UV-divergence $\omega(G)$ also specifies the superficial IR-divergence. A diagram has a superficial UV-divergence for $\omega(G) \geq 0$, and a superficial IR-divergence for $\omega(G) \leq 0$. The last of the $L+1$ integrations in a logarithmically IR-divergent diagram, with zero masses and external momenta, is always of the form:

$$\int \frac{d^D p}{(\mathbf{p}^2)^{2+L\varepsilon/2}} \,. \tag{12.9}$$

This integral is of the massless tadpole type considered in Eq. (8.33), which is equal to zero for any power $2 + L\varepsilon/2$ in dimensional regularization. It is UV-divergent for $D \geq 4 + L\varepsilon$, and IR-divergent for $D \leq 4 + L\varepsilon$. Dimensional regularization provides us with an analytic extrapolation of all Feynman integrals to dimensions $D < 4$, which produces pole terms $1/\varepsilon^i$. The IR-divergences occuring in massless Feynman integrals at $D = 4$ give rise to similar pole terms. In the generic tadpole integral (12.9), the IR-divergence compensates completely the UV-divergence.

In contrast to this, one nonzero external momentum $\mathbf{k}$ entering a massless diagram changes (12.9) to

$$\int \frac{d^D p}{(\mathbf{p}-\mathbf{k})^2 (\mathbf{p}^2)^{1+L\varepsilon/2}} \,. \tag{12.10}$$

Now the integral is IR-convergent, whereas the UV-divergence is unchanged. This is how a nonzero external momentum guarantees superficial IR-convergence of a massless Feynman integral. The lines through which the external momentum flows can be chosen rather arbitrarily. One may even modify the character of the vertices without changing the divergences: they must no longer be all of the ϕ^4-type, but can become ϕ^3-, ϕ^2-, and even ϕ^5-vertices. Examples are shown in Figs. 12.2 and 12.4.

Applying the method of *IR-rearrangement* (IRR), one nonzero external momentum supplies a convenient infrared cutoff, thus making the mass in the Feynman integral superfluous. The resulting zero-mass momentum space integrals consist of a massless $(L-1)$-loop insertion in a one-loop diagram as pictured in Fig. 12.1 [4]. They will generically be referred to as *propagator-type* or shorter *p-integrals*. A detailed discussion will be given in Chapter 13, in particular the powerful algorithms developed [5] for their calculation.

The rearrangement of the momentum is shown explicitly in Fig. 12.2. With IR-rearrangement, five-loop calculations up to $O(\varepsilon^{-1})$ can be reduced to a four-loop calculation up to $O(\varepsilon^0)$. The last integration generates a pole in ε (see 13.1.1).

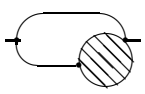

FIGURE 12.1 Generic propagator-type diagram obtained after infrared rearrangement as in Fig. 12.2.

While the introduction of a nonzero external momentum eliminates superficial IR-divergences, it does not in general guarantee the absence of IR-subdivergences. On page 199 we saw that diagrams with nonexceptional external momenta are free of IR-subdivergences.

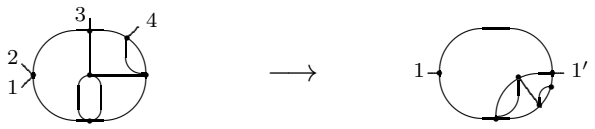

FIGURE 12.2 Simplification of massless Feynman integral by infrared rearrangement (IRR). Setting the external momenta 2 and 4 equal to zero leads to a diagram of the propagator type, corresponding to a one-loop diagram with an $(L-1)$-loop insertion, pictured in Fig. 12.1. Note the IR-rearrangement produces an artificial ϕ^3-vertex.

But after the rearrangement of the external momentum, they will in most cases be exceptional. Thus we have to check carefully to see whether an IR-divergence has been created by the rearrangement. This is facilitated by Eq. (12.7), which has to be modified to account for the possible existence of artificial ϕ^2-, ϕ^3-, and ϕ^5-vertices generated by the rearrangement. As an example, see the artificial ϕ^3-vertex generated in Fig. 12.2. If the rearranged diagram possesses V_r vertices of the ϕ^r-type for $r = 2, 3, 5$, we find the degree of superficial IR-divergence

$$\tilde{\omega}(\tilde{\gamma}) = -L(\tilde{\gamma})(D-4) - n + 2V_2 + V_3 - V_5, \tag{12.11}$$

where n is the number of external lines of the subdiagram. This expression implies an IR-divergence of the Feynman integral for $D = 4$, if there are n ϕ^3-vertices or $n/2$ ϕ^2-vertices in the shrunk diagram. Remember that in the shrunk diagrams all lines with an IR-cutoff, a mass, or an external momentum are shrunk. A ϕ^2-vertex always implies an IR-subdivergence in $D = 4$ forming a subdiagram with $n = 2$, such that $\omega = 0$. Up to five loops, all but two of the encountered IR-subdivergences are caused by this subdiagram, which is diagrammatically denoted as  , symbolizing an integral over $1/\mathbf{p}^4$. One subdiagram even occurs which contains two ϕ^2-vertices, which has $\tilde{\omega}(\gamma) = 2$. This subdiagram is  , corresponding to an integration over $1/\mathbf{p}^6$. Furthermore, IR-divergences are caused by subdiagrams with at least two ϕ^3-vertices for $n = 2$ and four ϕ^3-vertices for $n = 4$. In these cases $\tilde{\omega}(\gamma) = 0$. We shall not encounter subdiagrams with more ϕ^3-vertices than that. Examples containing IR-divergent subdiagrams will be considered in Subsection 12.4.2. The result of these considerations is that propagator-type integrals generated by infrared rearrangement are superficially IR-convergent at $D = 4$ as long as IR-rearrangement generates no IR-subdivergences with virtual vertices of the ϕ^2-type, or subdiagrams with two or four such vertices of the ϕ^3-type.

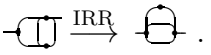

FIGURE 12.3 Simple example for generation of an IR-subdivergence by IR-rearrangement. In the integral on the left-hand side, the external momenta are reduced to a single momentum. The rearrangement produces an IR-divergence.

A simple example for the generation of an IR-subdivergence by IR-rearrangement is shown in Fig. 12.3. The associated Feynman integrals before and after rearrangement can be calculated without infrared rearrangement:

$$\int \frac{d^Dp\, d^Dq}{(2\pi)^{2D}} \frac{1}{\mathbf{q}^2(\mathbf{p}-\mathbf{q})^2(\mathbf{p}-\mathbf{k})^2\mathbf{p}^2} \xrightarrow{\text{IRR}} \int \frac{d^Dp\, d^Dq}{(2\pi)^{2D}} \frac{1}{(\mathbf{q}-\mathbf{k})^2(\mathbf{p}-\mathbf{q})^2\mathbf{p}^4}. \tag{12.12}$$

The removal of the IR-divergence of the IR-rearranged diagram on the right-hand side will be carried out in detail in Section 12.4.

As mentioned at the beginning of this chapter, sometimes infrared rearrangement generates calculable subdiagrams only if IR-subdivergences are admitted. An example for such a drastic version of infrared rearrangement [2] is displayed in Fig. 12.4. Here the integration over the

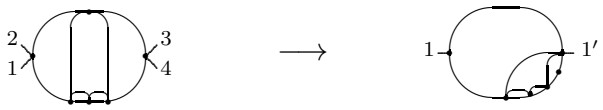

FIGURE 12.4 Simplification of massless Feynman integral by infrared rearrangement (IRR), generating an IR-divergence in a subdiagram. Setting the external momenta 2, 3, 4 to zero, and importing a nonzero external momentum $1'$, generates a one-loop diagram with a four-loop insertion. Unfortunately, an IR-divergence also arises from the newly created ϕ^2-vertex in the line below $1'$, which must be properly subtracted to obtain the correct UV-divergences.

massless line with the ϕ^2-vertex introduces the artificial IR-divergence which must be calculated and removed from the total divergence to find the correct UV-divergence. The subtraction will be done recursively in Section 12.4.

12.2.1 The R-Operation for Massless Diagrams

If the masses are set equal to zero, an important simplification occurs in the subtraction of quadratically divergent subdiagrams. The $\bar{R}$-operation involves subtractions of both logarithmically divergent and quadratically divergent subdiagrams, to be denoted by γ_4 and γ_2, respectively:

$$\bar{R}G = \sum_{\bar{\Gamma}} \prod_{\gamma_4 \in \bar{\Gamma}} (-\mathcal{K}\bar{R}\gamma_4) \prod_{\gamma_2 \in \bar{\Gamma}} (-\mathcal{K}\bar{R}\gamma_2) * (G/\bar{\Gamma}) \; . \tag{12.13}$$

For zero mass, the counterterms $\mathcal{K}\bar{R}\gamma_2$ of the quadratically divergent subdiagrams γ_2 are proportional to $\mathbf{p}^2$ only, where $\mathbf{p}$ is the momentum flowing through γ_2. As an example, consider the following Feynman integral where the four external momenta are replaced by only two:

$$G = \quad = \int \frac{d^D p}{(2\pi)^D} \frac{\gamma_2(\mathbf{p})}{\mathbf{p}^4 (\mathbf{p}-\mathbf{k})^2}, \tag{12.14}$$

and which contains the quadratically divergent subdiagram divergence

$$\gamma_2(\mathbf{p}) = \quad , \tag{12.15}$$

whose superficial divergence is given by

$$-\mathcal{K}\bar{R}(\quad) = \mathcal{Z}_{\gamma_2}(\varepsilon^{-1})\, \mathbf{p}^2. \tag{12.16}$$

The external square momentum $\mathbf{p}^2$ of the subdiagram is part of the integrand of the remaining integral. In the zero-mass case, it cancels a propagator in the denominator of the integrand, i.e., a line in the shrunk integral. The associated counterterm is then calculated as follows:

$$\Delta_{\gamma_2}(\mathbf{p}) * (G/\gamma_2) \quad = \quad -\mathcal{K}\bar{R}(\quad) * \quad \tag{12.17}$$

$$\equiv \int \frac{d^D p}{(2\pi)^D} \frac{\mathcal{Z}_{\gamma_2}(\varepsilon^{-1})\,\mathbf{p}^2}{\mathbf{p}^4(\mathbf{p}-\mathbf{k})^2}$$

$$= \mathcal{Z}_{\gamma_2}(\varepsilon^{-1}) \int \frac{d^D p}{(2\pi)^D} \frac{1}{\mathbf{p}^2(\mathbf{p}-\mathbf{k})^2}. \tag{12.18}$$

According to Eq. (12.16), the pole terms $\mathcal{Z}_{\gamma_2}(\varepsilon^{-1})$ may be considered as being obtained from the derivative of $-\mathcal{K}\bar{R}($ $)$ with respect to $\mathbf{p}^2$ as (recall the discussion in Section 11.8)

$$\mathcal{Z}_{\gamma_2}(\varepsilon^{-1}) = \partial_{\mathbf{p}^2} \mathcal{K}\bar{R}\gamma_2\,, \tag{12.19}$$

where the differentiation symbol $\partial_{\mathbf{p}^2} \equiv \partial/\partial\mathbf{p}^2$ acts only on the first expression to its right. Thus we may rewrite (12.18) as

$$\Delta_{\gamma_2}(\mathbf{p}) * (G/\gamma_2) = \mathcal{Z}_{\gamma_2}(\varepsilon^{-1})$$ 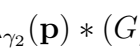 .

For any massless quadratically divergent diagram, the operation $*$ can be replaced by $\partial_{\mathbf{p}^2}$ acting on the pole term to its left, with a simultaneous removal of an associated propagator in the shrunk diagram to its right. From the point of view of the subdiagram, whose pole term is specified by $\partial_{\mathbf{p}^2}\mathcal{K}\bar{R}(\gamma_2)$, the internal momentum $\mathbf{p}$ of the total diagram is really an external momentum. Since we generally use the notation $\mathbf{k}$ rather than $\mathbf{p}$ to specify external momenta, we shall henceforth denote the pole terms by $\partial_{\mathbf{k}^2}\mathcal{K}\bar{R}(\gamma_2)$ for the sake of a more consistent notation.

Remember that due to the relation $\mathcal{K}\bar{R}\gamma_4 = \mathcal{Z}_{\gamma_4}(\varepsilon^{-1})$, the operation $*$ in logarithmically divergent subdiagrams reduces to a pure multiplication [see Eq. (11.5)]. For this reason, most of our recursive formulas will no longer contain the operation symbols $*$.

As a more complicated example, in which the above diagram appears as a subdiagram, consider the five-loop four-point diagram

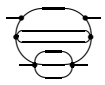 .

This diagram is very hard to calculate even with zero masses, if the external momenta are not rearranged. This will become clear in the next chapter. By setting the external momenta entering through the lower lines equal to zero, the pole terms of this diagram are equal to those of the infrared-rearranged diagram

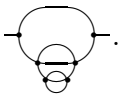 .

Application of the $\mathcal{K}\bar{R}$-operation yields the following expansion

$\mathcal{K}\bar{R}\Big($ 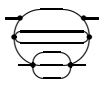 $\Big) = \mathcal{K}\bar{R}\Big($ 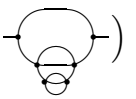 $\Big) = \mathcal{K}\Big[$ 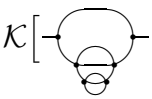 $- \partial_{\mathbf{k}^2}\mathcal{K}($  $)$ $- \partial_{\mathbf{k}^2}\mathcal{K}\bar{R}($ 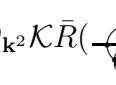 $)$ $\Big]$.

In the complete list of recursive diagrammatic expansions in Appendix A, this appears on page 420 as No. 15.

The propagator-type integrals appearing on the right-hand side are easy to calculate. A nonzero external momentum is assumed to enter through the two remaining external lines, thereby avoiding an IR-divergence in the upper loop. The rearranged diagram is IR-convergent because of the cancellation of one momentum square in the denominator of the quadratically divergent four-loop subdiagram.

12.2.2 Zero-Mass Simplifications for Z_ϕ

The counterterm contribution to Z_ϕ can be calculated from the tadpole-free two-point diagrams with zero mass. Up to four loops, this calculation is a rather straightforward application of the algorithm to be described in Chapter 13. At five loops, however, some non-standard techniques must be used. One of them is based on the possibility of transforming quadratically into logarithmically divergent diagrams by carrying out the differentiation with respect to the external momentum of Section 11.8. Setting the mass equal to zero in the differentiated integrals simplifies the expressions considerably. For $m = 0$, the derivatives (11.47) and (11.48) become

$$\frac{\partial}{\partial k_\mu}\frac{1}{(\mathbf{p}-\mathbf{k})^2} = -\frac{2(p-k)_\mu}{[(\mathbf{p}-\mathbf{k})^2]^2} = 2 \quad , \tag{12.21}$$

$$\frac{\partial^2}{\partial k_\mu \partial k_\mu}\frac{1}{(\mathbf{p}-\mathbf{k})^2} = \frac{-2D}{[(\mathbf{p}-\mathbf{k})^2]^2} + \frac{8}{[(\mathbf{p}-\mathbf{k})^2]^2} = \frac{2\varepsilon}{[(\mathbf{p}-\mathbf{k})^2]^2} = -2\varepsilon \quad . \tag{12.22}$$

Application to more than one propagator leads to a sum of terms:

$$\begin{aligned}\frac{\partial^2}{\partial k_\mu \partial k_\mu}\frac{1}{(\mathbf{p}-\mathbf{k})^2(\mathbf{q}-\mathbf{k})^2} &= 2\frac{\partial}{\partial k_\mu}\left\{\frac{(p-k)_\mu}{[(\mathbf{p}-\mathbf{k})^2]^2(\mathbf{q}-\mathbf{k})^2} + \frac{(q-k)_\mu}{(\mathbf{p}-\mathbf{k})^2[(\mathbf{q}-\mathbf{k})^2]^2}\right\} \\ &= \frac{-2D+8}{[(\mathbf{p}-\mathbf{k})^2]^2(\mathbf{q}-\mathbf{k})^2} + \frac{-2D+8}{(\mathbf{p}-\mathbf{k})^2[(\mathbf{q}-\mathbf{k})^2]^2} + \frac{8(p-k)_\mu(q-k)_\mu}{[(\mathbf{p}-\mathbf{k})^2]^2[(\mathbf{q}-\mathbf{k})^2]^2} \\ &= 2\,\varepsilon\left(- \quad - \quad \right) + 8\left(\right) .\end{aligned} \tag{12.23}$$

The dotted lines indicate propagators $1/(\mathbf{p}-\mathbf{q})^2$ entering into the vertices. These propagators are not written down explicitly to save space. After the differentiation, quadratically divergent diagrams have become logarithmically divergent.

Note that not all of the new logarithmically divergent diagrams are equivalent to four-point diagrams, as shown by an example. Let us calculate the counterterm contribution to Z_ϕ of the following five-loop diagram using $\partial/\partial\mathbf{k}^2 = (8-2\varepsilon)^{-1}\partial^2/\partial k_\mu \partial k_\mu$:

$$\begin{aligned}\mathcal{K}\bar{R}\left[\frac{\partial}{\partial \mathbf{k}^2}\Big(\Big)\right] &= \mathcal{K}\bar{R}\left[\frac{1}{8-2\varepsilon}\frac{\partial^2}{\partial k_\mu \partial k_\mu}\Big(\Big)\right] \\ &= \mathcal{K}\bar{R}\left[\frac{1}{8-2\varepsilon}\Big(-2\times 2\varepsilon \quad + 8 \quad \Big)\right] .\end{aligned} \tag{12.24}$$

The left of the two final diagrams is a four-point diagram with an artificial IR-divergence for zero mass. This divergence can be avoided by rearranging the flow of external momentum, which brings (12.24) to the form

$$\mathcal{K}\bar{R}\left[\frac{1}{8-2\varepsilon}\Big(-2\times 2\varepsilon \quad + 8 \quad \Big)\right] .$$

The resulting propagator-type integral is easy to calculate by the methods to be explained in the Chapter 13.

The second diagram on the right-hand side contains extra vertices and propagators with vector indices. Such diagrams will generically be called *diagrams with vector indices*. Due to the zero mass, the Feynman integrals of such diagrams can often be calculated quite simply

with the help of momentum conservation and directional averages. This will now be shown in an example. A further example will be given later in Eqs. (13.36) and (13.37), when illustrating another important calculation technique based on partial integrations of Feynman integrals in momentum space.

The momentum conservation at the vertices allows us to reduce some diagrams with vector indices to ordinary scalar integrals. This requires the introduction of directed lines. Consider the three-loop ϕ^4-diagram

G: 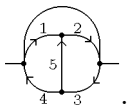

. (12.25)

The numbers on the lines label the momenta flowing through them. At the lowest vertex, momentum conservation implies

$$\mathbf{p}_3 = \mathbf{p}_4 + \mathbf{p}_5 \;\Rightarrow\; 2\,\mathbf{p}_3\cdot\mathbf{p}_4 = \mathbf{p}_3^2 + \mathbf{p}_4^2 - \mathbf{p}_5^2\,. \tag{12.26}$$

Inserting this into the integrand gives

$$\frac{p_{3\mu}p_{4\mu}}{\mathbf{p}_1^2\mathbf{p}_2^2\mathbf{p}_3^2\mathbf{p}_4^2\mathbf{p}_5^2} = \frac{1}{2}\left(\frac{1}{\mathbf{p}_1^2\mathbf{p}_2^2\mathbf{p}_4^2\mathbf{p}_5^2} + \frac{1}{\mathbf{p}_1^2\mathbf{p}_2^2\mathbf{p}_3^2\mathbf{p}_5^2} - \frac{1}{\mathbf{p}_1^2\mathbf{p}_2^2\mathbf{p}_3^2\mathbf{p}_4^2}\right), \tag{12.27}$$

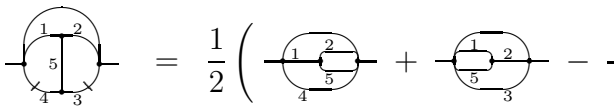

(12.28)

A canceled squared momentum in the denominator corresponds diagrammatically to a shrunk line.

For diagrams containing ϕ^4-vertices, the expansion of the type (12.27) is not always possible. As an example, take the last integral arising in the differentiation

$\mathcal{K}\bar{R}\left[\frac{\partial}{\partial\mathbf{k}^2}\left(\right.\right.$  $\left.\left.\right)\right] = \mathcal{K}\left[\frac{1}{8-2\varepsilon}\left(-2\varepsilon\bar{R}\right.\right.$  $- 2\varepsilon\bar{R}$  $\left.\left.+\,8\bar{R}\right.\right.$  $\left.\left.\right)\right]$. (12.29)

The differentiation generates two logarithmically divergent diagrams, which can be viewed as four-point diagrams with a zero external momentum entering at the ϕ^2-vertex. For zero mass, these ϕ^2-vertices create IR-divergences which are avoided by IR-rearrangement. The external momentum is rearranged such that it enters into the ϕ^2-vertex. In this way we replace (12.29) by

$\mathcal{K}\left[\frac{1}{4-\varepsilon}\left(-\varepsilon\bar{R}\right.\right.$  $- \varepsilon\bar{R}$  $\left.\left.+\,4\bar{R}\right.\right.$  $\left.\left.\right)\right]$. (12.30)

The third diagram on the right-hand side has propagators with vector indices which cannot be expanded as in (12.27), thus requiring a more complicated explicit calculation involving the different vector components.

12.3 Infrared Divergences in Dimensional Regularization

Before entering the general discussion on the subtraction of infrared divergences, let us first discuss their appearance in a few explicit Feynman integrals regularized by analytic continuation. They will illustrate, in particular, that zero masses alone are not sufficient to give rise

to $1/\varepsilon$-pole terms, unless the momenta are exceptional. Zero masses lead, in general, to singularities in $D-2$, D, $D+2, \ldots$. Poles in ε arise only after IR-rearrangement of the massless diagrams.

12.3.1 Nonexceptional External Momenta

As a first example, consider the logarithmically UV-divergent one-loop integral  , which was calculated in dimensional regularization in Eq. (8.63). Setting $m = 0$ in Eq. (8.67) leads to

$$\left.\vcenter{\hbox{  }}\right|_{m=0} = (\mu^\varepsilon g)^2 \frac{\Gamma(\varepsilon/2)}{(4\pi)^{D/2}} (\mathbf{k}^2)^{D/2-2} \int_0^1 dt\, [t\,(1-t)]^{D/2-2}\,. \tag{12.31}$$

Using the integral representation for the Beta function [compare (8.8)]

$$B(a,b) = \int_0^1 dt\, t^{a-1}(1-t)^{b-1} = \frac{\Gamma(a)\Gamma(b)}{\Gamma(a+b)} \tag{12.32}$$

we obtain

$$\left.\vcenter{\hbox{  }}\right|_{m=0} = (\mu^\varepsilon g)^2 \frac{\Gamma(\varepsilon/2)}{(4\pi)^{D/2}}\, (\mathbf{k}^2)^{D/2-2}\, \frac{\Gamma(D/2-1)\Gamma(D/2-1)}{\Gamma(D-2)}\,. \tag{12.33}$$

The first Gamma function $\Gamma(\varepsilon/2)$ contains the $1/\varepsilon$-pole term caused by the UV-divergence. Setting the mass equal to zero leads to additional divergences at the endpoints of the t-integral in (12.31) [which are absent for $m \neq 0$ in Eq. (8.67)]. These divergences appear as poles in the Beta function at $D = 2, 0, -2, \ldots$. The integral is IR-convergent for $D = 4$. Note that the single nonzero external momentum in this diagram is certainly nonexceptional (recall the definition on page 140).

12.3.2 Exceptional External Momenta

In the case of exceptional external momenta, we do find IR-divergence for $D = 4$ and $m = 0$. The example in Eq. (12.3) contains an integration over the ϕ^2-vertex:

$$\vcenter{\hbox{  }} \sim \int \frac{d^D p}{(2\pi)^D} \frac{1}{(\mathbf{p}^2+m^2)^2[(\mathbf{p}-\mathbf{k})^2+m^2]}\,. \tag{12.34}$$

Using the integral formula Eq. (8.69) for $a = 2$ and $b = 1$, we find

$$\vcenter{\hbox{  }} \propto \frac{\Gamma(3-D/2)}{(4\pi)^{D/2}\Gamma(2)\Gamma(1)} \int_0^1 dx\, x^0 (1-x)^1 \left[\mathbf{k}^2 x(1-x)+m^2\right]^{D/2-3}\,. \tag{12.35}$$

The integral is UV-divergent for $D \geq 6$. The integration over x is convergent as long as $m \neq 0$. If the mass is zero, it is IR-divergent for $D \leq 4$:

$$\begin{aligned} \left.\vcenter{\hbox{  }}\right|_{m=0} &= -(\mu^\varepsilon g)^2 \frac{\Gamma(3-D/2)(\mathbf{k}^2)^{D/2-3}}{(4\pi)^{D/2}} \int_0^1 dx\, x^{D/2-3}(1-x)^{D/2-2}. \\ &= -(\mu^\varepsilon g)^2 \frac{\Gamma(3-D/2)(\mathbf{k}^2)^{D/2-3}}{(4\pi)^{D/2}} \frac{\Gamma(D/2-2)\Gamma(D/2-1)}{\Gamma(D-3)}\,. \end{aligned} \tag{12.36}$$

The IR-divergence leads to poles at $D = 4, 2, \ldots$; the UV-divergence to poles at $D = 6, 8, \ldots$.

12.3.3 Massless Tadpole Diagrams

An important reason for setting all masses equal to zero was the fact that, in the minimal subtraction scheme, all integrals with tadpole parts (8.33) do not contribute to the counterterms (see Sections 11.7-11.8).

As an example, consider the quadratically divergent one-loop diagram  , which was found in Eq. (8.57) to give

$$\underset{\bullet}{\bigcirc} = -\mu^{\varepsilon} g \int \frac{d^D p}{(2\pi)^D} \frac{1}{\mathbf{p}^2 + m^2} = -\mu^{\varepsilon} g \frac{(m^2)^{D/2-1}}{(4\pi)^{D/2}} \Gamma(1 - D/2). \tag{12.37}$$

For $D > 2$, this vanishes in the limit $m \to 0$, such that we may set the dimensionally regularized integral $\int d^D p\, \mathbf{p}^{-2}$ equal to zero, as stated in Eq. (8.31). The example shows nicely that dimensional regularization controls IR-divergences in the same analytic way as UV-divergences, the two canceling each other for zero mass. This is an important property of the scheme. It allows us to calculate the UV-divergences of massive Feynman integrals from appropriately subtracted massless integrals, which are much easier to perform.

12.4 Subtraction of UV- and IR-divergences: R^*-Operation

From now on we shall deal exclusively with massless, mostly IR-rearranged diagrams. In order to find the correct counterterms produced by such diagrams at each order in perturbation theory, we introduce a generalization of the R-operation, called R^*-operation [2, 3], which subtracts UV-divergences as well as the artificial IR-divergences by IR-counterterms. The specification of the latter is based on an important difference between the two divergences: a superficial UV-divergence receives contributions from *all* lines of a loop. This is not the case for an IR-divergence where only massless lines contribute, and among these, only those which become singular at the same point in momentum space. We shall refer to such lines as not carrying external momentum. Whereas UV-divergences are subtracted loop by loop, IR-divergences are subtracted line by line, to be cut out of a loop. This fact will somewhat complicate the substitution of the IR-counterterm of the IR-divergent integrations.

In Subsection 12.4.1, an example for a simple R^*-operation is given. It illustrates the definition of the IR-divergent subdiagrams in the Subsection 12.4.2. Note that in the following the coupling constants as well as the factor $1/(2\pi)^2$ accompanying each coupling constant will be omitted.

12.4.1 Example for Subtraction of IR- and UV-Divergences

Consider the following logarithmically UV-divergent diagram 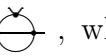 , which gives rise to the UV-divergent counterterms

$$\mathcal{K}\bar{R}\left(\text{  }\right) = \mathcal{K}\left[\text{  } - \mathcal{K}\left(\text{}\right) * \text{}\right]. \tag{12.38}$$

By IR-rearrangement, the diagram can be tranformed into 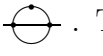 . This contains an additional IR-subdivergence which can be subtracted from  to obtain the correct UV-counterterms. The extra IR-subdivergence in the Feynman integral $\int d^D p\, [\mathbf{p}^4 (\mathbf{p} - \mathbf{q})^2]^{-1}$ is caused by the integral over $1/\mathbf{p}^4$ implied by the upper loop. The propagator $1/(\mathbf{p} - \mathbf{q})^2$ in the lower loop does not produce any IR-divergence. In calculating the IR-pole term, this propagator is nevertheless needed as an UV-cutoff, otherwise the UV-divergence would cancel the IR-divergence and

disappear from the integral, since the integral over $1/\mathbf{p}^4$ is a massless tadpole integral giving zero in dimensional integration.

In order to set us an iterative subtraction procedure, the extra IR-divergences will be isolated diagrammatically. The contribution of the upper loop integral in  has near $D = 4$ dimensions the form:

$$\mathcal{K}(\;\;) = \mathcal{K}\left(\int d^Dp\,[\mathbf{p}^4(\mathbf{p}-\mathbf{q})^2]^{-1}\right) \propto \frac{1}{\varepsilon}\frac{1}{\mathbf{q}^2}, \tag{12.39}$$

with a constant proportionality factor. The resulting $1/\mathbf{q}^2$ on the right-hand side of (12.39) plays the role of a second propagator in the lower loop integral of 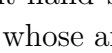 , whose analytic form is $\int d^Dq\,[\mathbf{q}^2(\mathbf{q}-\mathbf{k})^2]^{-1}$. The latter integral is the same as for a Feynman diagram  evaluated at zero external momentum.

At first one may be tempted to represent the IR-divergence by a diagram such as $\mathcal{K}($  $)$. This would be misleading, since the upper line of the right-hand diagram is really the result of the left-hand diagram, so that this line is counted twice. This could be saved by employing the symbolic notation $\mathbf{q}^2\,\mathcal{K}($  $)$ for the divergence. This, however, is not recommendable for another reason. The factor in the integrand causing the IR-divergence, here $1/\mathbf{p}^4$, produces $1/\varepsilon^i$-pole terms which are independent of the original Feynman integral. Examples for diagrams in which $1/\mathbf{p}^4$ appears in different loop diagrams will be shown for a different purpose in Fig. 12.5. This independence makes it preferable to set up a diagrammatic notation exhibiting directly the IR-divergent part of the integral as the factor. In the present case, we represent the IR-divergence caused by the integrand $1/\mathbf{p}^4$ as follows: [6]

$$-\mathbf{q}^2\,\mathcal{K}(\;\;) = \left(\;\;\right)_{IR}\;. \tag{12.40}$$

The small open circles at the end of the vertical line indicate vertices at which the line is connected to the initial diagram. With this notation, the diagrammatic formulation of all subtractions is

$$\mathcal{K}\bar{R}^*\left(\;\;\right) = \mathcal{K}\left\{\;\; + \left(\;\;\right)_{IR}\;\; - \mathcal{K}(\;\;)\left[\;\; + \left(\;\;\right)_{IR}\right]\right\}. \tag{12.41}$$

This produces the same result as in the purely ultraviolet subtraction procedure for massive propagators in Eq. (12.38). There are two IR-subtractions, one for the full two-loop diagram and one for the UV-subtracted subdiagram. The second term on the right-hand side subtracts a pure IR-divergence. The third term vanishes because the remaining diagram is of the massless tadpole type, being zero in dimensional regularization. The last term subtracts an IR- as well as a UV-divergence. Obviously, the calculation of the IR-subtraction terms and their combination with the rest of a diagram are more complicated than in the ultraviolet case.

The calculation of massless diagrams has so far been possible up to five loops, and will be discussed in the next chapter. For the present discussion of IR-subtractions we anticipate the following general formula:

$$\mathbf{k}\;\overset{a}{\underset{b}{\bigcirc}}\;\sim \frac{\Gamma(D/2-a)\Gamma(D/2-b)\Gamma(a+b-D/2)}{(4\pi)^{-\varepsilon/2}\,\Gamma(a)\Gamma(b)\Gamma(D-a-b)}\frac{1}{(\mathbf{k}^2)^{a+b-D/2}}\,, \tag{12.42}$$

where a and b are the powers of the propagators. For $a = b = 1$, we find the following small-ε expansion:

$$\bigcirc = \frac{1}{\varepsilon} + 2 - \gamma - \log\frac{\mathbf{k}^2}{4\pi\mu^2} + \mathcal{O}(\varepsilon)\,. \tag{12.43}$$

This expansion agrees with the result for the massive integral in Eq. (8.68), setting $m = 0$ and $\psi(1) = -\gamma$.

The explicit pole term for the IR-divergence is then

$$\mathcal{K}\Big(\quad\Big) = -\frac{2}{\varepsilon}\frac{1}{\mathbf{q}^2}. \tag{12.44}$$

As mentioned before, the propagator $1/(\mathbf{p}-\mathbf{q})^2$ does not contribute to the IR-divergence, but acts as UV-cutoff, thereby generating a factor $1/\mathbf{q}^2$:

$$\Big(\quad\Big)_{IR} = -\mathbf{q}^2\mathcal{K}\Big(\quad\Big) = \frac{2}{\varepsilon}\,. \tag{12.45}$$

This pole term multiplies the remaining loop integral .

The diagrammatic subtraction of UV- and IR-divergences differs in an important point. A UV-divergence is caused by a loop integral in a subdiagram which is shrunk to a virtual vertex after the integration. For the IR-divergences, on the other hand, not all the lines of a loop integral are relevant. In contrast to the UV-divergence, the lines responsible for the IR-divergence are not shrunk to a point, but removed from the diagram. This process yields the full subtraction term:

$$\mathcal{K}\left[\Big(\quad\Big)_{IR}\quad\right] = \mathcal{K}\left[\frac{2}{\varepsilon}\int\frac{d^Dq}{(2\pi)^D}\frac{1}{\mathbf{q}^2(\mathbf{q}-\mathbf{k})^2}\right] = \frac{2}{\varepsilon^2}+\frac{4}{\varepsilon}-\frac{2}{\varepsilon}\gamma-\frac{2}{\varepsilon}\log\frac{\mathbf{k}^2}{4\pi\mu^2}\,. \tag{12.46}$$

Omitting the vanishing tadpole term in the $\bar{R}^*$-operation in Eq. (12.41), the explicit calculation of the UV-counterterms of the diagram involves the following three subtractions, separated by square brackets in the second line:

$$\begin{aligned}
\mathcal{K}\bar{R}^*\Big(\quad\Big) &= \mathcal{K}\Big[\qquad\qquad + \Big(\quad\Big)_{IR}\qquad\qquad - \Big(\quad\Big)_{IR}\mathcal{K}\Big(\quad\Big)\Big] \\
&= \left[-\frac{2}{\varepsilon^2}-\frac{3}{\varepsilon}+\frac{2}{\varepsilon}\left(\gamma+\log\frac{\mathbf{k}^2}{4\pi\mu^2}\right)\right]+\left[\frac{4}{\varepsilon^2}+\frac{4}{\varepsilon}-\frac{2}{\varepsilon}\left(\gamma+\log\frac{\mathbf{k}^2}{4\pi\mu^2}\right)\right]-\left[\frac{4}{\varepsilon^2}\right] \\
&= -\frac{2}{\varepsilon^2}+\frac{1}{\varepsilon}\,.
\end{aligned} \tag{12.47}$$

For comparison, the calculation of these counterterms from the $\bar{R}$-operation applied to the massive diagram in Eq. (12.38), goes as follows:

$$\begin{aligned}
\mathcal{K}\bar{R}\Big(\quad\Big) &= \mathcal{K}\Big[\qquad\qquad - \quad\mathcal{K}\Big(\quad\Big)*\quad\Big] \\
&= \left[\frac{2}{\varepsilon^2}+\frac{5}{\varepsilon}-\frac{2}{\varepsilon}\left(\gamma+\log\frac{\mathbf{k}^2}{4\pi\mu^2}\right)\right] - \left[\frac{4}{\varepsilon^2}+\frac{4}{\varepsilon}-\frac{2}{\varepsilon}\left(\gamma+\log\frac{\mathbf{k}^2}{4\pi\mu^2}\right)\right] \\
&= -\frac{2}{\varepsilon^2}+\frac{1}{\varepsilon}\,.
\end{aligned} \tag{12.48}$$

In order to generalize this diagrammatic subtraction procedure, some new notations must be introduced.

12.4.2 Graph-Theoretic Notations

First, we must properly identify IR-divergent subdiagrams of a diagram G. As observed above, there is an important difference between UV- and IR-divergent subdiagrams. In the first case,

subdiagrams are complete 1PI ϕ^4-diagrams. They form closed loops, in which all lines contribute to the UV-divergence. Taking the UV-divergent subintegration out of the diagram is diagrammatically represented by shrinking its loops.

In contrast to this, the IR-divergent subdiagrams are not 1PI subdiagrams of the ϕ^4-theory, Their lines do not form closed loops. All lines which carry momentum of the remaining diagram do not contribute to the IR-divergence. This is why the removal of IR-divergent subintegration from a diagram will be represented diagrammatically by cutting the responsible lines out of the subdiagram. The rules for doing this are:

- A *subdiagram* γ contributing with all of its lines to an IR-divergence is separated from the remaining diagram by cutting one or several loops. The corresponding loop momenta become external momenta in γ. The vertices, at which γ is connected to G, are drawn as hollow circles.

- The *subtracted diagram* or *remaining diagram* $\hat{\gamma} = G\backslash\gamma$ is created from G by taking away the lines and internal vertex points of γ. The integration connecting γ and $G\backslash\gamma$ is omitted, and the corresponding loop momenta play the role of external momenta in γ as well as $\hat{\gamma}$.

- The *contracted subdiagram* $\tilde{\gamma} = G/\hat{\gamma}$ is formed from G by shrinking the lines of $\hat{\gamma}$ to a point. Alternatively, the diagram $\tilde{\gamma}$ is obtained from γ by contracting the vertices which connect γ to $\hat{\gamma}$, and which are represented by open circles, to a single vertex. Note that different subdiagrams γ can produce the same $\tilde{\gamma}$.

Let I_γ be the integrand of γ, and $\mathbf{k} = \mathbf{k}_1, \ldots, \mathbf{k}_n$ the external momenta of G. Further let $\mathbf{p} = \mathbf{p}_1, \ldots, \mathbf{p}_N$ be the common external momenta of γ and $\hat{\gamma}$, which are the momenta of the loops to be cut out of the diagram G, and $\mathbf{l} = \mathbf{l}_1, \ldots, \mathbf{l}_{L(\gamma)}$ and $\mathbf{q} = \mathbf{q}_1, \ldots, \mathbf{q}_m$ be the internal momenta of γ and $\hat{\gamma}$, respectively. Then we find for the above-defined quantities the general analytic expressions:

$$G(\mathbf{k}) \;\propto\; \int d^Dp\, d^Dq\, d^Dl\, I_\gamma(\mathbf{l},\mathbf{p}) I_{\hat{\gamma}}(\mathbf{q},\mathbf{p},\mathbf{k}), \tag{12.49}$$

$$\gamma(\mathbf{p}) \;\propto\; \int d^Dl\, I_\gamma(\mathbf{l},\mathbf{p}), \tag{12.50}$$

$$\hat{\gamma}(\mathbf{p},\mathbf{k}) = G\backslash\gamma(\mathbf{p},\mathbf{k}) \;\propto\; \int d^Dq\, I_{\hat{\gamma}}(\mathbf{q},\mathbf{p},\mathbf{k}), \tag{12.51}$$

$$\tilde{\gamma} \;\propto\; \int d^Dp\, I_{\gamma(\mathbf{p})}. \tag{12.52}$$

The definitions will be illustrated by the following examples. The hollow circles in γ and in $\tilde{\gamma}$ indicate the vertices connecting γ and $\hat{\gamma}$, which are contracted to a single point in $\tilde{\gamma}$.

Example 1: $G =$  , $\gamma =$  $\Rightarrow \hat{\gamma} =$  $\tilde{\gamma} =$  .

Example 2: $G =$  , $\gamma =$  $\Rightarrow \hat{\gamma} =$  $\tilde{\gamma} =$  .

Example 3: $G =$  , $\gamma =$  $\Rightarrow \hat{\gamma} =$  , $\tilde{\gamma} =$  .

The three examples illustrate an important role of $\tilde{\gamma}$. The diagrams γ and $\tilde{\gamma}$ contain the same lines. But $\tilde{\gamma}$ contains, in addition, an integral over all external momenta of γ, such that $\tilde{\gamma}$ has the same Feynman integral as a vacuum diagram. Sometimes the diagrams $\tilde{\gamma}$ contain

cutvertices, which arise from the contraction of the vertices in $\hat{\gamma}$. The loop diagrams separated by these cutvertices are formed by the lines carrying the momenta of $\hat{\gamma}$, which are the external momenta of the subdiagram γ. The number of external momenta N of γ is thus given by:

$$N = L(\tilde{\gamma}) - L(\gamma). \tag{12.53}$$

The external momenta in $\tilde{\gamma}$ provide an IR-cutoff for the integrations of γ. A cutvertex in $\tilde{\gamma}$ separates loops whose lines contribute to IR-divergences at different points in the momentum space. Something similar happens when external momentum $\mathbf{k}$ of the full diagram G flows into one of the inner vertices of γ, because the lines through which $\mathbf{k}$ flows also contribute to an IR-divergence at a different point in momentum space. The external momentum may well flow through all lines of γ, just as in the shrunk diagram $\tilde{\gamma}$ on page 200. A somewhat artificial example for this case is $G =$  , where both lines, the upper and the lower one, contribute independently to an IR-divergence, but not both together since the external momentum in one of the lines prevents them from getting singular at the same point in momentum space.

We are now ready to define the subdiagrams whose IR-divergences have to be subtracted. A subdiagram $\gamma \subset G$ is called *infrared irreducible* (IRI) if

1. the associated contracted subdiagram $\tilde{\gamma} = G/\hat{\gamma}$ contains no cutvertex,

2. no external momentum of G flows into an internal vertex of the subdiagram γ, i.e., if external momentum flows either through *all* lines of γ or through *none* of them, and

3. the subdiagram γ contains only massless lines.

If all three conditions are satisfied, each line of the subdiagram γ contributes to the IR-divergence of the integrations of $\tilde{\gamma}$.

Among the above examples, only the first one is IRI, and only if the external momentum of G flows entirely through $\hat{\gamma}$. The IRI subdiagrams play the same role for IR-divergences as the 1PI subdiagrams for the UV-divergences. The IR-divergences come exclusively from IR-divergent IRI subdiagrams.

An IRI subdiagram is said to be IR-divergent if its superficial degree of IR-divergence is $\tilde{\omega}(\gamma) \geq 0$.

$$\begin{aligned} \tilde{\omega}(\gamma) &= \omega(\hat{\gamma}) - \omega(G) = 4L(\hat{\gamma}) - 2I(\hat{\gamma}) - 4L(G) + 2I(G) \\ &= -[4L(\tilde{\gamma}) - 2I(\tilde{\gamma}))] = -\omega(\tilde{\gamma})\,. \end{aligned} \tag{12.54}$$

This definition coincides with the previous one in Eq. (12.7). In our applications, $\tilde{\omega}$ will be nonzero only once: $\tilde{\omega}\Big($  $\Big) = 2$. There is one five-loop diagram, in which this subdiagram appears and cannot be avoided by any trick.

A set of IR-divergent IRI subdiagrams $\{\gamma_i\}$ is said to be *IR-disjoint* in G if

(i) the subdiagrams are pairwise non-overlapping, and

(ii) no IRI subdiagram *in* G can be composed from them.

Diagrams which are IR-disjoint contribute independently to IR-divergences, by analogy with UV-disjoint diagrams. Their selection prevents double subtractions in the recursive definition of the IR-counterterms.

By analogy with the definition of the sets in Eq. (11.1),

$$\Gamma = \{\gamma | \gamma \in G, \gamma \text{ UV-disjoint}\}, \tag{12.55}$$

we define the sets Γ', which contain the IR-divergent IRI subdiagrams of G:

$$\Gamma'(G) = \{\gamma' | \gamma' \subset G, \gamma' \text{ IR-disjoint}\} \; . \tag{12.56}$$

Examples of the set of all possible sets Γ' for two different diagrams transformed by IR-rearrangement are shown in Fig. 12.5. The subtraction of all UV- and IR-divergences of a diagram G will involve all sets Γ and Γ' contained in G.

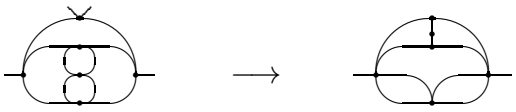

$\{\text{all possible } \Gamma'(G)\}$ = 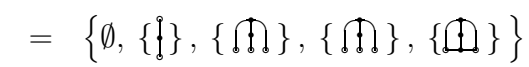

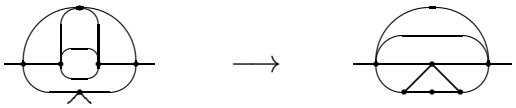

$\{\text{all possible } \Gamma'\}$ = 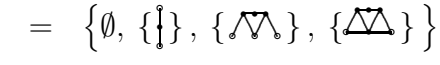

FIGURE 12.5 All possible sets of infrared-disjoint subdiagrams for two diagrams transformed by infrared rearrangement.

12.4.3 Definition of R^*- and $\bar{R}^*$-Operation

For a systematic recursive subtraction of the artificial IR-divergences in massless Feynman diagrams, the R-operation defined in Eqs. (11.3)–(11.13) is extended to an R^*-operation [2, 3]. The subtraction is possible because the UV- and IR-divergences originate from different regions in momentum space, which yield clearly distinguishable additive contributions. For any diagram G, the R^*-operation yields a finite result:

$$\mathcal{K} R^* \, G \; = \; 0 \, . \tag{12.57}$$

The operation is a sum over all possible terms in which UV- and IR-divergent subintegrations γ and γ' are replaced by the corresponding pole terms with the help of Δ_γ and $\Delta'_{\tilde{\gamma'}}$:

$$\begin{aligned} \mathcal{K} R^* \, G \; &= \; \sum_{\Gamma \cap \Gamma' = 0} \prod_{\gamma' \in \Gamma'} \Delta'_{\tilde{\gamma'}} * \prod_{\gamma \in \Gamma} \Delta_\gamma * G \backslash \Gamma' / \Gamma \\ &= \; \sum_{\Gamma \cap \Gamma' = 0} \Delta'_{\Gamma'} * \Delta_\Gamma * G \backslash \Gamma' / \Gamma \; , \end{aligned} \tag{12.58}$$

where $\Delta'_{\Gamma'}$ is defined in terms of the IR-disjoint subdiagrams γ' in the same way as Δ_Γ was in terms of the UV-disjoint subdiagrams γ in Eq. (11.8):

$$\Delta'_{\Gamma'} \equiv \prod_{\gamma' \in \Gamma'} \Delta'_{\tilde{\gamma'}} . \tag{12.59}$$

The operations $*$ insert Δ_γ and $\Delta'_{\tilde{\gamma}'}$ into the remaining integration. We use $\tilde{\gamma}$ as a subscript of Δ', because it contains all IR-divergent loop integrations, and because different subdiagrams γ may lead to the same $\tilde{\gamma}$ and $\Delta'_{\tilde{\gamma}}$. The sums over all Γ and Γ' with $\Gamma \cap \Gamma' = 0$ guarantee that all subdivergences are subtracted, and that no oversubtractions occur. Since the sum runs over nonoverlapping sets Γ and Γ', the shrinking and the removal of the corresponding subdiagrams in G can be done in an arbitrary order:

$$G\backslash\Gamma'/\Gamma = G/\Gamma\backslash\Gamma'.$$

The Feynman diagrams to be calculated are not superficially IR-divergent because an external momentum is used as an IR-cutoff. Therefore, the term which contains the superficial IR-divergence of G vanishes:

$$\Delta'_G * G\backslash G = \Delta'_G = 0.$$

The superficial UV-divergence, the UV-counterterm, is therefore calculated as follows:

$$\Delta_G \;=\; \sum_{\bar{\Gamma}\cap\bar{\Gamma}'=0} \Delta'_{\bar{\Gamma}'} * \Delta_{\bar{\Gamma}} * G\backslash\bar{\Gamma}'/\bar{\Gamma} \;\equiv\; -\mathcal{K}\bar{R}^* G\,. \tag{12.60}$$

In general, the operators Δ_Γ and $\Delta'_{\Gamma'}$ do not commute because of their momentum dependence. The UV-divergence has to be subtracted first. However, for logarithmically divergent subdiagrams where $\tilde{\omega}(\gamma) = 0$, the operators commute. This is the most common case. An example with $\tilde{\omega}(\gamma) > 0$ will be discussed in detail below.

The UV-divergent subdiagrams of an IR-divergent diagram may contain IR-divergences. The counterterm is therefore determined with

$$\Delta_\gamma = -\mathcal{K}\bar{R}^*\gamma. \tag{12.61}$$

The subdiagrams in the five-loop calculation have at most four loops. All their counterterms can be calculated without introducing IR-divergences, such that the extension to the $\bar{R}^*$-operation is superfluous, and we may apply the recursive operation $\bar{R}$ only:

$$\Delta_\gamma = -\mathcal{K}\bar{R}\,\gamma\,. \tag{12.62}$$

12.4.4 Construction of Infrared Subtraction Terms of Subdiagrams

Formally, IR-subtraction terms in the sum (12.60) look very similar to UV-subtraction terms:

$$\Delta'_{\tilde{\gamma}'} * G\backslash\gamma'\,. \tag{12.63}$$

However, they involve completely different procedures. First, the action of the operator $\Delta'_{\tilde{\gamma}'}$ is completely different, since it inserts a pole term rather than an IR-divergent subintegration as in the UV-case. Second, the formation of the remaining diagram $G\backslash\gamma'$ is different. The reason for these differences is that the previous UV-divergences are caused by *all* lines of a loop, such that the full loop integral must be subtracted. In contrast, the IR-divergence is caused only by one or a few lines of a loop. Thus the IR-divergent subdiagram γ is only a part of an integrand, which is connected to the remaining diagram by an integration. When replacing the subdiagram by the corresponding pole term, this integration has still to be carried out, and this has an effect on the remaining diagram if $\tilde{\omega}(\gamma) \neq 0$, unless the result of the integration is a constant.

If the IR-divergent subdiagram consists only of a single line and involves no loop, for example $\gamma = 1/\mathbf{p}^4$ in (12.12) with $\tilde{\omega}(\gamma) = 0$, the subtraction term is simple. It contains the pole term

$\mathcal{Z}'_{\tilde\gamma}(\varepsilon^{-1})$ instead of the integrand γ. The diagrammatic notation for this pole term is $(\gamma)_{IR}$. The integration over the momentum $\mathbf{p}$ is taken care of by inserting a factor $\delta^{(D)}(\mathbf{p})$, thus ensuring that the remaining integral is evaluated for $\mathbf{p}=0$ where the IR-divergence is generated:

$$\Delta'_{\tilde\gamma} * G\backslash\gamma = \mathcal{Z}'_{\tilde\gamma}(\varepsilon^{-1}) \int \frac{d^Dp}{(2\pi)^D}(2\pi)^D\delta^{(D)}(\mathbf{p})\ \hat\gamma(\mathbf{p},\mathbf{k})\,, \qquad \tilde\omega(\gamma)=0,\ L(\gamma)=0\,. \tag{12.64}$$

In the general case, an IRI subdiagram γ of G has internal loops and more than one loop connecting it with the subtracted diagram $\hat\gamma = G\backslash\gamma$. The notation for the momenta will be the same as in Section 12.4.2, with loop momenta of γ labeled by $\mathbf{l}=(\mathbf{l}_1,\dots,\mathbf{l}_{L(\gamma)})$, and the N external momenta of γ and of $\hat\gamma$ by $\mathbf{p}=(\mathbf{p}_1,\dots,\mathbf{p}_N)$. The loop momenta of $\tilde\gamma$ are $\mathbf{p}'=(\mathbf{p}'_1,\dots,\mathbf{p}'_{\tilde\gamma})$. By construction, the momenta $\mathbf{p}'$ comprise all $\mathbf{p}$ and $\mathbf{l}$, i.e., $\mathbf{p}'=(\mathbf{p},\mathbf{l})$. The integrand represented by $\tilde\gamma$ or γ is called $I_{\tilde\gamma}=I_\gamma$. The integral associated with the full diagram G is, in this notation:

$$G(\mathbf{k}) = \int \frac{d^Dp}{(2\pi)^D}\frac{d^Dl}{(2\pi)^D}\left[\hat\gamma(\mathbf{p},\mathbf{k})\right] I_{\tilde\gamma}(\mathbf{p},\mathbf{l})\,. \tag{12.65}$$

An example is displayed in Fig. 12.6.

$G(\mathbf{k})$ $\gamma(\mathbf{p})$ $\hat\gamma(\mathbf{k},\mathbf{p})$ $\tilde\gamma$

FIGURE 12.6 The inner momenta of γ are called $\mathbf{l}_1,\ \mathbf{l}_2$. The contracted subdiagram $\tilde\gamma$ contains, in addition, the integration over $\mathbf{p}$. The IR-divergence occurs for vanishing momenta $\mathbf{l}_1,\ \mathbf{l}_2,\ \mathbf{p}$.

In general, the operator $\Delta'_{\tilde\gamma}$ acts on G by incorporating the counterterm for γ into the integral:

$$\Delta'_{\tilde\gamma} * G\backslash\gamma = \int \frac{d^Dp}{(2\pi)^D}\frac{d^Dl}{(2\pi)^D}\left[\hat\gamma(\mathbf{k},\mathbf{p})\right]\Delta'_{\tilde\gamma}(\mathbf{p},\mathbf{l})\,. \tag{12.66}$$

The operator $\Delta'_{\tilde\gamma}(\mathbf{p},\mathbf{l})$ is defined as a local expression which isolates the IR-divergences:

$$\Delta'_{\tilde\gamma}(\mathbf{p}') = \mathcal{P}'_{\tilde\gamma}\left(\frac{\partial}{\partial\mathbf{p}'}\right)\prod_{i=1}^{L(\tilde\gamma)}(2\pi)^D\,\delta^{(D)}(p'_i)\,, \tag{12.67}$$

where $\mathcal{P}'_{\tilde\gamma}$ is a homogeneous polynomial of degree $\tilde\omega(\gamma)$ in $(\partial/\partial\mathbf{p}'_1,\dots,\partial/\partial\mathbf{p}'_{L(\tilde\gamma)})$, with ε-dependent coefficients. They are pure pole terms in the MS-scheme:

$$\mathcal{K}\,\mathcal{P}_{\tilde\gamma} = \mathcal{P}_{\tilde\gamma}\,. \tag{12.68}$$

They are uniquely defined by requiring that $\mathcal{K}R^*\,G$ in Eq. (12.58) be finite. The differentiations applied to the δ-functions can be moved around in the integral by partial integrations. Since these do not generate surface terms in dimensionally regularized integrals, the differentiations act on those lines of $\hat\gamma$ through which flows an external momentum of γ. The differentiations generate the same powers of the associated momenta as would arise from carrying out the integration over the external and internal momenta of γ.

In the calculations of the diagrams in this text, we have encountered only two simple cases: most frequently, the subdiagrams are logarithmically divergent with $\tilde\omega(\gamma)=0$ for an arbitrary number of external momenta N [recall (12.53)]. The operator is then simply given by

$$\Delta'_{\tilde\gamma}(\mathbf{p}) = \mathcal{Z}'_{\tilde\gamma}\prod_{i=1}^{L(\tilde\gamma)}(2\pi)^D\,\delta^{(D)}(\mathbf{p}_i)\,. \tag{12.69}$$

Only do we encounter a quadratically IR-divergent subdiagram with $\tilde{\omega}(\gamma) = 2$ which has $N = 1$. There the operator is

$$\Delta'_{\tilde{\gamma}}(\mathbf{p}) = \mathcal{Z}'_{\tilde{\gamma}} \left(\frac{\partial}{\partial p_\mu}\right)^2 (2\pi)^D \, \delta^{(D)}(\mathbf{p}) \,. \tag{12.70}$$

It has been shown that none of the UV-and IR-pole terms of subdiagrams with L loops produce singularities which are for $\varepsilon \to 0$ more singular than $(\varepsilon^{-1})^L$ [3].

The general structure of the operator (12.67) can be understood better by the following consideration. The IR-divergent integration over γ in $D = 4 - \varepsilon$-dimensions is the integration over a four-dimensional pole in momentum space. The subtraction term is therefore constructed by replacing γ by the corresponding ε-pole term. This replacement is done at the point of the singularity in momentum space. The remaining term in G is the residue of the four-dimensional pole term. For an analytic function $f(z)$ with an isolated singularity at a and a Laurent expansion

$$f(z) = \sum_{n=-m}^{\infty} c_n (z-a)^n, \tag{12.71}$$

the residue c_{-1} is obtained by the operation:

$$(m-1)! \, c_{-1} = \left(\frac{d}{dz}\right)^{m-1} (z-a)^m f(z) \Bigg|_{z=a} . \tag{12.72}$$

The case of a simple pole with $m = 1$ leads to a logarithmic divergence and corresponds in four dimensions to $1/\mathbf{p}^4$ with $\tilde{\omega} = 0$. The case of $m = 3$ is a quadratic IR-divergence corresponding in four dimensions to $1/\mathbf{p}^6$ with $\tilde{\omega} = 2$. The number of the differentiations is given by the deviation from a logarithmic divergence. For the calculation of the residue in four dimensions, $m - 1$ is thus replaced by $\tilde{\omega}(\gamma)$:

$$\left(\frac{\partial}{\partial p_\mu}\right)^{\tilde{\omega}(\gamma)} \hat{\gamma}(\mathbf{p}, \mathbf{k}) \Bigg|_{\mathbf{p}=0} . \tag{12.73}$$

The IR-divergent poles $1/\mathbf{p}^4$ and $1/\mathbf{p}^6$ with $\tilde{\omega}(\gamma) = 0$ and $\tilde{\omega}(\gamma) = 2$, respectively, are subtracted with the help of the operator

$$\Delta'_{\tilde{\gamma}} * G \backslash \gamma = \mathcal{Z}'_{\tilde{\gamma}}(\varepsilon^{-1}) \int \frac{d^D p}{(2\pi)^D} (2\pi)^D \delta^{(D)}(\mathbf{p}) \left(-\frac{\partial}{\partial p_\mu}\right)^{\tilde{\omega}} \hat{\gamma}(\mathbf{p}, \mathbf{k}) \,. \tag{12.74}$$

Let us discuss some examples in detail:

Example 1: The diagram

$G =$ 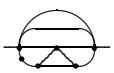 $\sim \int \frac{d^D p}{(2\pi)^D} \frac{\hat{\gamma}(\mathbf{p}, \mathbf{k})}{\mathbf{p}^4}$ (12.75)

contains the same IR-divergent subdiagram $\gamma =$  with $\tilde{\omega}(\gamma) = 0$ as the example discussed in Subsection 12.4.1. The counterterm is constructed with the help of the generic expression (12.64). The resulting IR-pole term was calculated before in (12.45): $\mathcal{Z}'_\gamma(\varepsilon^{-1}) = 2/\varepsilon$. Here the IR-divergent $\mathbf{p}$-integral contains three different propagators:

$$\int \frac{d^D p}{(2\pi)^D} \frac{1}{\mathbf{p}^4 (\mathbf{p} - \mathbf{q}_1)^2 (\mathbf{p} - \mathbf{q}_2)^2}. \tag{12.76}$$

The δ-function in the $\mathbf{p}$-integral of the generic expression (12.64) forces $\mathbf{p}$ to be zero in $1/(\mathbf{p}-\mathbf{q}_1)^2(\mathbf{p}-\mathbf{q}_2)^2$, such that in the remaining diagram these propagators may simply be replaced by $1/\mathbf{q}_1^2\mathbf{q}_2^2$. The subtraction term and its diagrammatic notation are then

$$\Delta'_\gamma * G\backslash\gamma = \int \frac{d^Dp}{(2\pi)^D}\, \mathcal{Z}'(\varepsilon^{-1})\, (2\pi)^D\delta^{(D)}(\mathbf{p})\, \hat{\gamma}(\mathbf{p},\mathbf{k}) = \Big(\quad\Big)_{IR}$$  (12.77)

The $\bar{R}^*$-operation of the entire diagram G will be given as an example at the end of the section.

Example 2: The following diagram G contains a subdiagram γ with $\tilde{\omega}(\gamma)=2$:

$G =$  $-, \quad \gamma =$  $\Rightarrow\ \hat{\gamma} =$  . (12.78)

The remaining diagram $\hat{\gamma}$ contains two propagators carrying the momentum of γ. The subtraction term is of the form:

$$\Delta'_\gamma * G\backslash\gamma = \mathcal{Z}'_{\tilde{\gamma}}(\varepsilon^{-1})\Big(\frac{\partial^2}{\partial p_\mu \partial p_\mu}\, G\backslash\gamma\Big)\Big|_{\mathbf{p}=0}. \tag{12.79}$$

The momentum differentiations in Δ'_γ are carried out when incorporating the counterterm in $\hat{\gamma}$. Since

$$\frac{\partial^2}{\partial p_\mu \partial p_\mu}\,\frac{1}{(\mathbf{p}-\mathbf{q}_1)^2(\mathbf{p}-\mathbf{q}_2)^2} = \frac{2\varepsilon}{(\mathbf{p}-\mathbf{q}_1)^4(\mathbf{p}-\mathbf{q}_2)^2} + \frac{2\varepsilon}{(\mathbf{p}-\mathbf{q}_1)^2(\mathbf{p}-\mathbf{q}_2)^4} + \frac{8(p-q_1)_\mu(p-q_2)_\mu}{(\mathbf{p}-\mathbf{q}_1)^4(\mathbf{p}-\mathbf{q}_2)^4}, \tag{12.80}$$

the incorporation proceeds diagrammatically as follows:

$\Delta'_\gamma * G\backslash\gamma \;=\; \Big(\quad\Big)_{IR} *$

$\;=\; \mathcal{Z}'_{\tilde{\gamma}}(\varepsilon^{-1}) \cdot \Big(2\varepsilon$  $+\, 2\varepsilon$ $+\, 8$ $\Big)$. (12.81)

Example 3: Consider a quadratically IR-divergent subdiagram with a UV-divergent remaining diagram. The incorporation of an IR-counterterm with $\tilde{\omega}(\gamma) > 0$ changes drastically the subtracted diagram. Here the order in which the UV- and IR-divergences are subtracted is very important. The calculation of the counterterm of the logarithmically divergent diagram of Eq. (12.18) in the last section via the R-operation has the diagrammatic representation:

$\mathcal{K}\bar{R}\Big($  $\Big) = \mathcal{K}\Big[$ $- \partial_{\mathbf{k}^2}\mathcal{K}($  $)$ $\Big]$, (12.82)

with the operation $\partial_{\mathbf{k}^2}\mathcal{K}$ defined in Subsection 12.2.1. The UV-divergent subdiagram has $\omega(\gamma)$=2, such that the insertion of $\Delta_\gamma(\mathbf{p})$ into the shrunk diagram cancels a line.

Alternatively, the counterterm can be determined in a somewhat more complicated manner by applying the $\bar{R}^*$-operation to the following diagram G:

$G =$, $\gamma =$ $\Rightarrow\ \hat{\gamma} =$  . (12.83)

It contains the same IRI subdiagram as the last example with $\tilde{\omega}(\gamma) = 2$, and a quadratically UV-divergent remaining diagram $\hat{\gamma}$. If the IR-divergences are subtracted first, the IR-counterterm $\left(\right)_{IR}$ must be incorporated into , leading to the multiplication of the pole term by the diagram $2\,\varepsilon$. The UV-divergence of this diagram

$$-\mathcal{K}\bar{R}^{*}\left(\right) = -\mathcal{K}\bar{R}\left(\right) \tag{12.84}$$

is not a UV-subdivergence of the original diagram. The subtraction of such a term would be wrong:

$$\mathcal{K}\bar{R}^{*}\left(\right) = \mathcal{K}\Big[\; + \left(\right)_{IR}\Big(2\varepsilon\; - \underbrace{2\varepsilon\,\mathcal{K}\bar{R}(\;)}_{\text{wrong}}\Big)\Big]\,. \tag{12.85}$$

The subdiagram in G from which the UV-counterterm really originates is $\gamma' =$. Therefore, if $\tilde{\omega}(\gamma) \neq 0$, the UV-terms have to be subtracted first, thus avoiding a change of the UV-behavior.

The UV-counterterm $\mathcal{K}(\;)$ has the explicit diagrammatic form $\mathcal{K}(\;) * \;$. This vanishes because of the tadpole part. Subtracting both the UV-divergence of with $\mathcal{K}(\;) = \mathcal{Z}_{\gamma'}(\varepsilon^{-1})\mathbf{p}^2$, and the IR-divergence of with $\left(\right)_{IR} = \mathcal{Z}'_{\tilde{\gamma}}$, gives

$$\begin{aligned}\Delta'(\gamma)\,\mathcal{K}(\;) &= \mathcal{Z}_{\gamma'}(\varepsilon^{-1})\int\frac{d^Dp}{(2\pi)^D}\left[\left(-\frac{\partial}{\partial\mathbf{p}}\right)^2\mathbf{p}^2\right]\delta^{(D)}(p)\,\mathcal{Z}'_{\tilde{\gamma}}(\varepsilon^{-1})\\ &= \mathcal{Z}_{\gamma'}(\varepsilon^{-1})\,\mathcal{Z}'_{\tilde{\gamma}}(\varepsilon^{-1})\cdot 2D\,.\end{aligned} \tag{12.86}$$

The correct $\bar{R}^{*}$-operation is

$$\mathcal{K}\bar{R}^{*}\left(\right) = \mathcal{K}\left[\; + \left(\right)_{IR}\cdot 2\varepsilon\; - \left(\right)_{IR}\cdot 2D\,\partial_{\mathbf{p}^2}\mathcal{K}(\;)\right]. \tag{12.87}$$

The five-loop calculations contain only one case where this special treatment is necessary: the diagram No. 116 in Appendix A on page 434. It can be calculated analytically only in the IR-rearranged form shown on the right hand side of Fig. 12.7. Here we have dealt only with the IRI subdiagram with $\tilde{\omega} = 2$, i.e., the type examined also in Examples 3 and 4. The full R^{*}-operation will be presented at the end of the section.

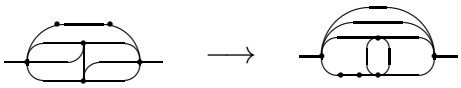

FIGURE 12.7 Infrared rearrangement of the special five-loop diagram No. 116 in Appendix A on page 434, whose IR-counterterm is calculated explicitly in Example 3, and whose complete R^{*}-operation is constructed in Section 12.5.

12.4.5 IR-Counterterms

The IR-counterterm of a diagram G can be calculated with the help of the general equation (12.60). The contribution from an IR-divergent subdiagram γ can be calculated using an arbitrary auxiliary diagram G_γ which contains γ and is superficially UV-convergent, i.e., which has $\Delta_{G_\gamma} = 0$. The IR-counterterm depends only on the integrand $I_{\tilde{\gamma}}(\mathbf{p},\mathbf{l})$ in (12.65), such that any G_γ can be used which leaves $I_{\tilde{\gamma}}(\mathbf{p},\mathbf{l})$ unchanged. The simplest G_γ is constructed by multiplying $I_{\tilde{\gamma}}(\mathbf{p},\mathbf{l})$ by $\prod_i^N[(\mathbf{p}_i-\mathbf{k})^2]^{-s_i}$ and integrating over $\mathbf{p}_i$ and $\mathbf{l}$. Diagrammatically, each

subdiagram $\hat{\gamma}$ is replaced by s_i lines for each loop connecting γ and $\hat{\gamma}$. The number of the connecting loops is N. As an example, we replace for $N = 1$ and $s = 1$:

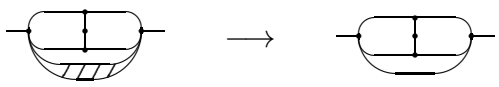

$$\int \frac{d^Dp}{(2\pi)^D}\frac{d^Dl}{(2\pi)^D}\;\hat{\gamma}(\mathbf{p},\mathbf{k})I_{\tilde{\gamma}}(\mathbf{p},\mathbf{l}) \;\longrightarrow\; \int \frac{d^Dp}{(2\pi)^D}\frac{d^Dl}{(2\pi)^D}\;\frac{I_{\tilde{\gamma}}(\mathbf{p},\mathbf{l})}{(\mathbf{p}-\mathbf{k})^2}\,. \tag{12.88}$$

The numbers s_i are chosen to make G_γ superficially UV-convergent:

$$\omega(G_\gamma) = \omega(\tilde{\gamma}) - 2\,s_i \;<\; 0\,. \tag{12.89}$$

For IR-divergent subdiagrams, $s_i = 1$ is in general sufficient. Up to the five-loop level, we shall find only one exception, where $s = 2$ is needed, with the associated IR-divergence complicating the calculation. The term in the R^*-operation of G_γ which subtracts the IR-divergence of γ is then [recall (12.67)]

$$\begin{aligned}\Delta'_{\tilde{\gamma}} * G_\gamma\backslash\gamma \;&=\; \mathcal{K}\int\frac{d^Dl}{(2\pi)^D}\prod_i^N\left\{\frac{d^Dp_i}{(2\pi)^D}\frac{1}{[(\mathbf{p}_i-\mathbf{k})^2]^{s_i}}\right\}\Delta'_{\tilde{\gamma}}(\mathbf{p}_i,\mathbf{l})\\ &=\; \mathcal{K}\,{\mathcal{P}'}_\gamma\left(-\frac{\partial}{\partial\mathbf{p}_i}\right)\prod_i^N\frac{1}{[(\mathbf{p}_i-\mathbf{k})^2]^{s_i}}\bigg|_{\mathbf{p}_i=0}\,.\end{aligned} \tag{12.90}$$

For $\omega(\tilde{\gamma}) = 0$, this simplifies to

$$\Delta'_{\tilde{\gamma}} * G_\gamma\backslash\gamma = \mathcal{Z}'_{\tilde{\gamma}}(\varepsilon^{-1})\;\frac{1}{(\mathbf{k}^2)^{\sum_i^N s_i}}; \tag{12.91}$$

and for $\omega(\tilde{\gamma}) = -2$ and $s = 1$, to

$$\Delta'_{\tilde{\gamma}} * G_\gamma\backslash\gamma = \mathcal{Z}'_{\tilde{\gamma}}(\varepsilon^{-1})\;\frac{2\varepsilon}{(\mathbf{k}^2)^{\sum_i^N s_i+1}}. \tag{12.92}$$

Now, the R^*-operation of G_γ is used to calculate $\Delta'_{\tilde{\gamma}} * G_\gamma\backslash\gamma$. Since G_γ is not superficially UV-divergent, we have $\Delta_{G_\gamma} = 0$, and since G_γ contains an external momentum, we have $\Delta'_{G_\gamma} = 0$. Therefore, we find:

$$\mathcal{K}\bar{R}^*\,G_\gamma = \mathcal{K}\left[f\Delta'_{\tilde{\gamma}} * G_\gamma\backslash\gamma + \sum_{\Gamma,\Gamma'\neq\gamma,G_\gamma}\Delta_\Gamma *\;\Delta'_{\Gamma'} * G_\gamma\backslash\Gamma'/\Gamma\right] = 0, \tag{12.93}$$

with a factor f counting how often $\Delta'_{\tilde{\gamma}} * G_\gamma\backslash\gamma$ is subtracted in the operation $\mathcal{K}\bar{R}^*\,G_\gamma$. In most cases, $f = 1$. A case with $f = 2$ occurs in Example 2 below. By construction of G_γ, we have $\mathcal{K}(\Delta'_{\tilde{\gamma}} * G_\gamma\backslash\gamma) = \Delta'_{\tilde{\gamma}} * G_\gamma\backslash\gamma$. We can thus obtain the IR-counterterms from the following operation:

$$\Delta'_{\tilde{\gamma}} * G_\gamma\backslash\gamma = -\frac{1}{f}\mathcal{K}\sum_{\Gamma,\Gamma'\neq\gamma,G_\gamma}\Delta_\Gamma *\;\Delta'_{\Gamma'} * G_\gamma\backslash\Gamma'/\Gamma \equiv -\frac{1}{f}\mathcal{K}\bar{\bar{R}}^*\,G_\gamma\,, \tag{12.94}$$

where the operator $\bar{\bar{R}}^*$ subtracts the UV- and IR-divergences of all subdiagrams excluding γ.

Combining this with Eq. (12.91), the IR-pole term for $\omega(\tilde{\gamma}) = 0$ is then calculated as

$$\mathcal{Z}'_{\tilde{\gamma}}(\varepsilon^{-1}) = -\frac{1}{f}(\mathbf{k}^2)^{\sum_i^N s_i}\mathcal{K}\bar{\bar{R}}^*\,G_\gamma. \tag{12.95}$$

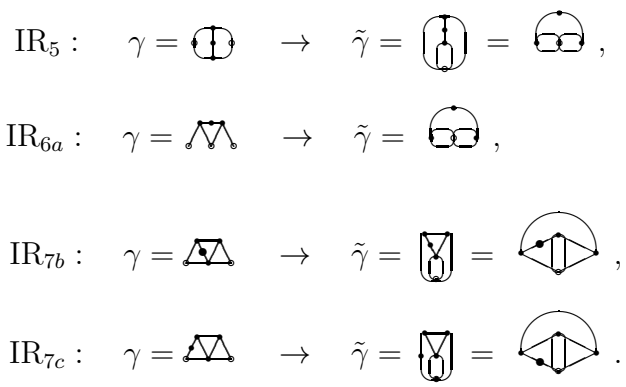

FIGURE 12.8 Typical infrared counterterms depending only on $\tilde{\gamma}$. We see that different IRI subdiagrams γ can have the same infrared counterterms.

In the R^*-operation, only the pole term $\mathcal{Z}'_{\tilde{\gamma}}(\varepsilon^{-1})$ is used. This pole term is called the IR-counterterm, and is denoted by $(\gamma)_{IR}$:

$$(\gamma)_{IR} = \mathcal{Z}'_{\tilde{\gamma}} = -\frac{1}{f}(\mathbf{k}^2)^{\Sigma_i^N s_i}\,\mathcal{K}\bar{\bar{R}}^*\,G_\gamma. \tag{12.96}$$

Although it is $\tilde{\gamma}$ which defines the divergence uniquely (see Fig. 12.8), the counterterm will be written as $(\gamma)_{IR}$ to simplify the notation. We now present a few sample calculations of counterterms.

Example 1: For the calculation of the IR-counterterm of the subdiagram $\gamma =$, we use the following G_γ:

$$G_\gamma =$$. (12.97)

The IR-divergent subdiagram is logarithmically divergent, i.e., $\omega(\tilde{\gamma}) = 0$.

In the ultraviolet, the diagram G_γ is convergent, with $\omega(G_\gamma) = -2$. Hence $\Delta_{G_\gamma} = 0$, and

$$\Delta'_{\tilde{\gamma}} * G_\gamma \backslash \gamma = \mathcal{Z}'_{\tilde{\gamma}}\,\frac{1}{\mathbf{k}^2} = -\mathcal{K}\bar{\bar{R}}^*\,G_\gamma = -\mathcal{K}\,G_\gamma. \tag{12.98}$$

The pole term is thus given by:

$$\Big($$ $\Big)_{\rm IR} = -\mathbf{k}^2\mathcal{K}\Big($$ $\Big) = -\mathbf{k}^2\mathcal{K}\int\frac{d^Dp}{(2\pi)^D}\frac{1}{\mathbf{p}^4(\mathbf{p}-\mathbf{k})^2} = \frac{2}{\varepsilon}\,.$ (12.99)

The above IR-counterterm may be used in various $\bar{R}^*$-operations, for instance in

$$\mathcal{K}\bar{R}^*\Big($$ 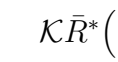 $\Big) = \mathcal{K}\Big[$ $+ \Big($  $\Big)_{IR} *$ $- \Big($ $\Big)_{IR} * \mathcal{K}($ $)\Big].$ (12.100)

The fully subtracted Feynman integral is

$$\begin{aligned}\mathcal{K}\bar{R}^*\Big($$ 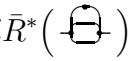 $\Big) \;=\; \mathcal{K}\Big[&\int\frac{d^Dp\,d^Dq}{(2\pi)^{2D}}\frac{1}{\mathbf{p}^4(\mathbf{p}-\mathbf{q})^2(\mathbf{q}-\mathbf{k})^2} \\ &+\Big(-\mathbf{k}^2\mathcal{K}\int\frac{d^Dp}{(2\pi)^D}\frac{1}{\mathbf{p}^4(\mathbf{p}-\mathbf{k})^2}\Big)\int\frac{d^Dq}{(2\pi)^D}\frac{1}{\mathbf{q}^2(\mathbf{q}-\mathbf{k})^2} \\ &-\Big(-\mathbf{k}^2\mathcal{K}\int\frac{d^Dp}{(2\pi)^D}\frac{1}{\mathbf{p}^4(\mathbf{p}-\mathbf{k})^2}\Big)\mathcal{K}\Big(\int\frac{d^Dq}{(2\pi)^D}\frac{1}{\mathbf{q}^2(\mathbf{q}-\mathbf{k})^2}\Big)\Big].\end{aligned} \tag{12.101}$$

Example 2: Let us also study a diagram with $f \neq 1$ in Eq. (12.94). The IR-counterterms required for the R^*-operation of the diagram in Fig. 12.6 need the determination of the counterterm associated with the following IR-divergent subdiagram:

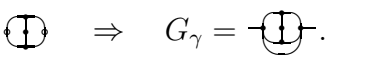

(12.102)

Since $\tilde{\omega} = 0$ and $s = 1$, the counterterm is given by

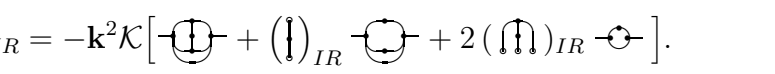

(12.103)

Note the factor 2 in the last term, since the corresponding IR-subdiagram appears twice in G_γ. This leads to a factor $f = 2$ in the associated IR-counterterm with the following G_γ:

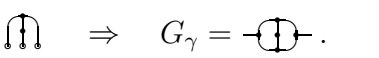

(12.104)

We have $N = 2$, and $\tilde{\omega} = 0$. In the $\bar{R}^*$-operation of G_γ, the same factor 2 appears:

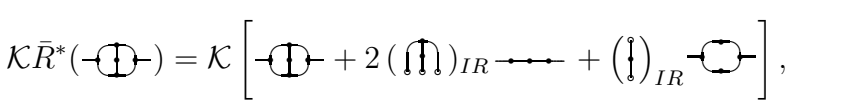

(12.105)

such that $f = 2$. The counterterm for $\gamma =$  is then calculated from

$$\begin{aligned} \Delta'_{\tilde{\gamma}} * G_\gamma \backslash \gamma &= \int \frac{d^D p_1\, d^D p_2}{(2\pi)^{2D}} \frac{\mathcal{Z}'_{\tilde{\gamma}}(\varepsilon^{-1})\ (2\pi)^{2D}\ \delta^{(D)}(p_1)\, \delta^{(D)}(p_2)}{(\mathbf{p}_1 - \mathbf{k})^2 (\mathbf{p}_2 - \mathbf{k})^2} \\ &= \mathcal{Z}'_{\tilde{\gamma}}(\varepsilon^{-1}) \frac{1}{\mathbf{k}^2}\,. \end{aligned} \tag{12.106}$$

This gives

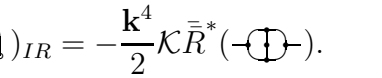

(12.107)

Example 3: For the subdiagram $\gamma =$  , we construct the auxiliary diagram G_γ as follows:

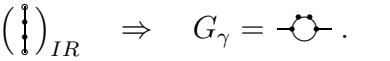

(12.108)

The IR-divergent subdiagram is quadratically IR-divergent, $\tilde{\omega}(\gamma) = 2$, whereas G_γ is UV-convergent, as it should, with $\omega(G_\gamma) = -4$. Hence $\Delta_{G_\gamma} = 0$, and

$$\Delta'_{\tilde{\gamma}} * G_\gamma = \mathcal{K}\Big[\mathcal{Z}'_{\tilde{\gamma}}(\varepsilon^{-1}) \frac{\partial^2}{\partial p_\mu \partial p_\mu} \frac{1}{[(\mathbf{p} - \mathbf{k})^2]^s}\Big|_{\mathbf{p}=0}\Big] = -\mathcal{K}\bar{\bar{R}}^*\, G_\gamma\,. \tag{12.109}$$

For $s = 1$,

$$\frac{\partial^2}{\partial p_\mu \partial p_\mu} \frac{1}{(\mathbf{k} - \mathbf{p})^2}\Big|_{\mathbf{p}=0} = \frac{2\varepsilon}{\mathbf{k}^4}\,, \tag{12.110}$$

and the pole in ε cancels:

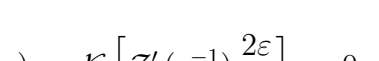

(12.111)

In the present case, a propagator $1/(\mathbf{p}-\mathbf{k})^2$ cannot be used. We have to choose $s=2$, giving

$$\frac{\partial^2}{\partial p_\mu \partial p_\mu}\,\frac{1}{(\mathbf{k}-\mathbf{p})^4}\bigg|_{\mathbf{p}=0} = \frac{8+4\varepsilon}{\mathbf{k}^6}\,, \tag{12.112}$$

leading to

$$\mathcal{K}\left[\mathcal{Z}'_{\tilde{\gamma}}(\varepsilon^{-1})\,\frac{8+4\varepsilon}{\mathbf{k}^6}\right] \;=\; -\mathcal{K}\bar{\bar{R}}^*\,G_\gamma = -\mathcal{K}\bar{\bar{R}}^*\,(\;\text{  }\;)\,. \tag{12.113}$$

As $\mathcal{Z}'_{\tilde{\gamma}}$ consists of at most a simple pole, it is found by

$$\Rightarrow \mathcal{K}\,\mathcal{Z}'_{\tilde{\gamma}}(\varepsilon^{-1}) \;=\; -\frac{\mathbf{k}^6}{8}\,\mathcal{K}\bar{\bar{R}}^*\,G_\gamma \tag{12.114}$$

$$\;=\; -\frac{\mathbf{k}^6}{8}\mathcal{K}\Big(\;\text{  }\;+\;\Big(\;\text{}\;\Big)_{IR} * \;\text{}\;\Big)$$

$$\;=\; -\frac{\mathbf{k}^6}{8}\mathcal{K}\left(\;\text{}\;+\;\Big(\;\text{}\;\Big)_{IR}\frac{1}{\mathbf{k}^6}\right) = \frac{1}{4\varepsilon}\,. \tag{12.115}$$

12.5 Examples for the $\bar{\bar{R}}^*$-Operation

We conclude this chapter by giving two examples for the complete R^*-operation. The first is typical for diagrams containing especially many IRI subdiagrams.

Diagram No. 53

Consider the diagram No. 53 on page 423 of Appendix A. Its IR-structure is rearranged for the calculation as follows:

(12.116)

This gives rise to IR-divergent IRI subdiagrams with up to three loops. The R^*-operation has the diagrammatic representation

$$\mathcal{K}\bar{R}^*\Big(\;\text{ 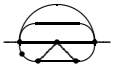 }\;\Big) \;=\; \mathcal{K}\Bigg[\;\text{ 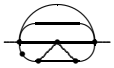 }\;+\;\Big(\;\text{}\;\Big)_{IR}\;\text{  }\;-\mathcal{K}\bar{R}^*(\;\text{  }\;)\Big(\;\text{}\;\Big)_{IR}$$

$$+(\;\text{}\;)_{IR}\;\text{  }\;-\mathcal{K}\bar{R}^*(\;\text{  }\;)(\;\text{}\;)_{IR}$$

$$+(\;\text{}\;)_{IR}\;\text{  }\;-\mathcal{K}\bar{R}(\;\text{  }\;)(\;\text{}\;)_{IR}$$

$$+\;(\;\text{}\;)_{IR}\;\text{}\;-\mathcal{K}(\;\text{}\;)(\;\text{}\;)_{IR}\Bigg]\,. \tag{12.117}$$

There is no term subtracting only a UV-divergence, as the corresponding shrunk diagram has a tadpole form and gives zero. The subtraction of the UV-subdivergences is simplified by IR-rearrangement:

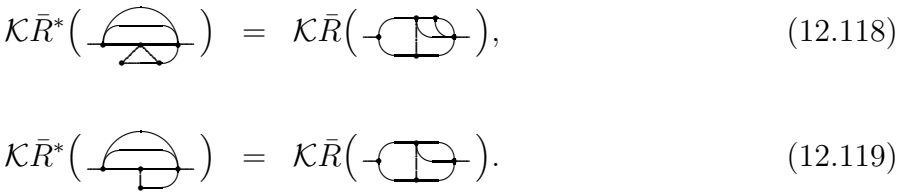

(12.118)

(12.119)

In the following, the subtraction terms of the UV-subdivergences are denoted directly by $\mathcal{K}\bar{R}(\gamma)$. All IR-counterterms have $\tilde{\omega}(\gamma) = 0$. The incorporation is again a simple multiplication, as in the previous Example 2:

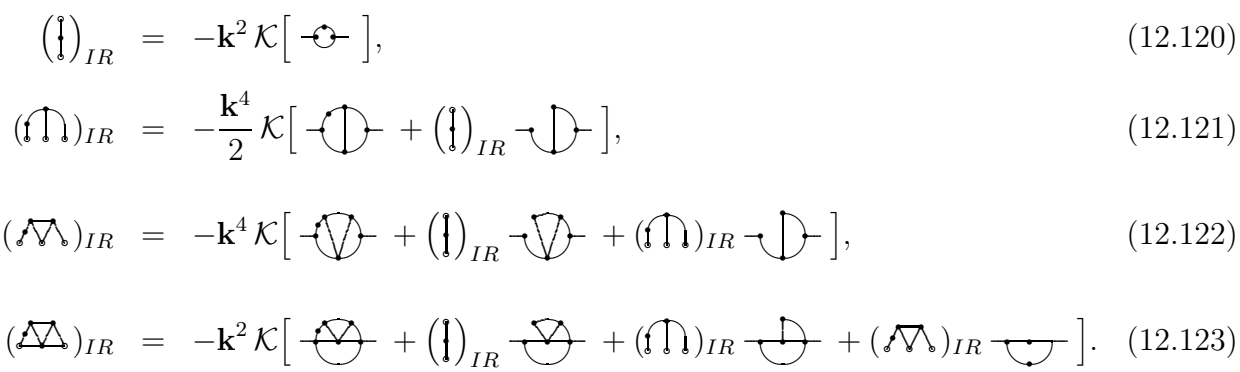

(12.120)

(12.121)

(12.122)

(12.123)

Diagram No. 116

As a second example, we choose the diagram No. 116 of Appendix A, page 434. Its IR-rearrangement was shown in Fig. 12.7. The R^*-operation of this diagram is exceptional, since it is the only case where an IRI subdiagram has $\tilde{\omega} = 2$. The subtraction of such a diagram requires differentiations in the remaining integral, thereby causing the non-commutativity of IR- and UV-subtractions. This problem was already illustrated in the second and third examples on page 217. The full R^*-Operation goes as follows:

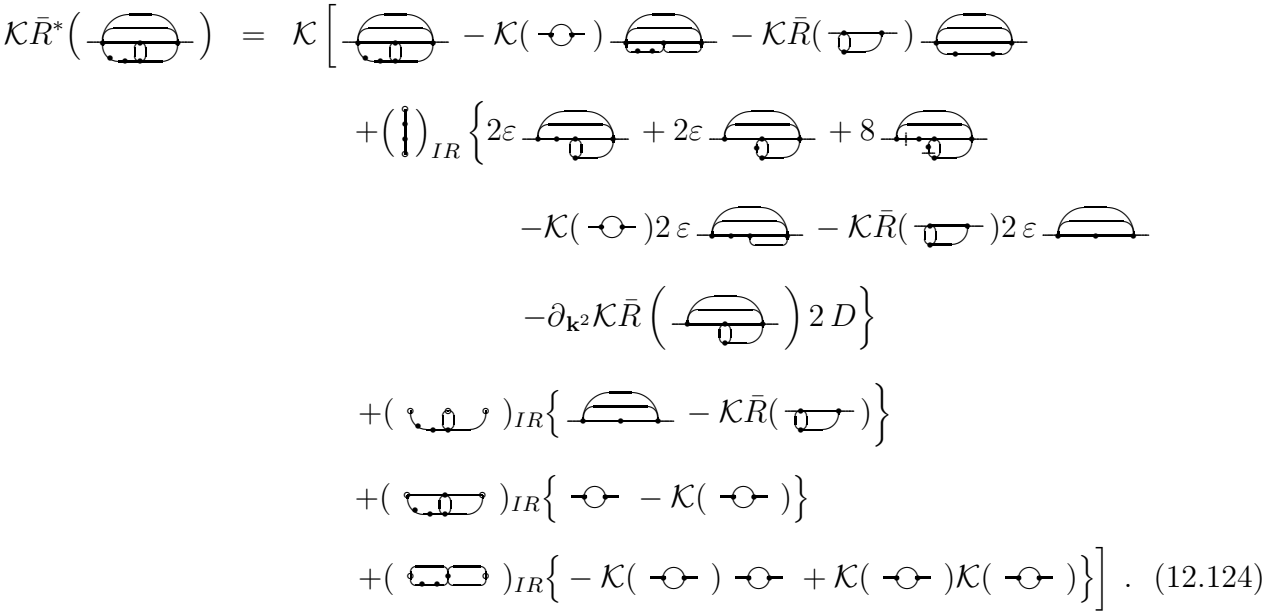

(12.124)

Note that, by analogy with Subsection 12.4.4, the term

$$2D\Big(\ \Big)_{IR}\,\partial_{\mathbf{k}^2}\mathcal{K}\bar{R}(\ \ )$$

is subtracted, not

$$2\varepsilon\,\Big(\ \Big)_{IR}\,\mathcal{K}\bar{R}(\ \ ).$$

Only the first term contains the UV-subdivergence of the diagram. The last term would have to be taken if the IR-subtractions had been carried out first and the UV-subtractions would be applied to the resulting terms (see the examples in Subsection 12.4.4).

The IR-counterterm with $\tilde{\omega} = 2$ was calculated in Eq. (12.115). The other counterterms have $\tilde{\omega} = 0$, and their pole terms are

$$(\ \ )_{IR} \;=\; -\mathbf{k}^4\,\mathcal{K}\Big[\ \ - \mathcal{K}(\ \ )\ \ - \mathcal{K}\bar{R}(\ \ )\ \ + \Big(\ \Big)_{IR}\Big\{2\,\varepsilon\ \ + 2\,\varepsilon\ \ - 2\,\varepsilon\mathcal{K}(\ \ )\ \ - 2\,\varepsilon\mathcal{K}\bar{R}(\ \ )\ \ + 8\ \ \Big\}\Big] \tag{12.125}$$

$$(\ \ )_{IR} \;=\; -\mathbf{k}^2\,\mathcal{K}\Big[\ \ - \mathcal{K}(\ \ )\ \ - \mathcal{K}\bar{R}(\ \ )\ \ + \Big(\ \Big)_{IR}\Big\{2\,\varepsilon\ \ + 2\,\varepsilon\ \ - 2\,\varepsilon\,\mathcal{K}(\ \ )\ \ - 2\,\varepsilon\,\mathcal{K}\bar{R}(\ \ )\ \ + 8\ \ \Big\} + (\ \ )_{IR}\Big\{-\mathcal{K}(\ \ )\ \ \Big\} + (\ \ )_{IR}\ \ \Big] \tag{12.126}$$

$$(\ \ )_{IR} \;=\; -\mathbf{k}^2\,\mathcal{K}\Big[\ \ - \mathcal{K}(\ \ )\ \ + \Big(\ \Big)_{IR}\Big\{2\,\varepsilon\ \ - 2\,\varepsilon\,\mathcal{K}(\ \ )\ \ \Big\}\Big] \tag{12.127}$$

Appendix 12A Proof of Interchangeability of Differentiation and $\bar{R}$-Operation

The proof is nontrivial because the operation $\bar{R}$ is defined for diagrams, whereas differentiation operators act on lines [7]. We proceed by induction in the number of loops. By the chain rule, differentiation of a diagram G involves a sum of differentiations for each line l of the diagram:

$$\partial G = \sum_l \partial_l G. \tag{12A.1}$$

If applied to a subdiagram γ, the line l may lie outside the subdiagram γ under consideration. In this case, we interchange the derivative with γ, i.e., $\partial\gamma = \gamma\partial$. This property will be needed below.

We want to show that $\partial\bar{R}G = \bar{R}\partial G$. The left-hand side is more explicitly

$$\begin{aligned}\partial\bar{R}G &= \partial \sum_{\Gamma(G)} \left(\prod_{\gamma\in\Gamma} -\mathcal{K}\bar{R}\gamma\right) G/\Gamma \\ &= \sum_{\Gamma(G)} \left[\partial\left(\prod_{\gamma\in\Gamma} -\mathcal{K}\bar{R}\gamma\right) G/\Gamma + \left(\prod_{\gamma\in\Gamma} -\mathcal{K}\bar{R}\gamma\right)\partial(G/\Gamma)\right].\end{aligned}$$

In applying ∂ to the product of factors $-\mathcal{K}\bar{R}\gamma$, we use the product rule, whereby ∂ can be interchanged with the operator $\mathcal{K}$ without problem. As an induction hypothesis, we assume that it also can be interchanged with γ, if γ is a proper subdiagram of G. This implies that $\partial\mathcal{K}\bar{R}\gamma = \mathcal{K}\bar{R}\partial\gamma$, and we find

$$\partial\bar{R}G = \sum_{\Gamma(G)} \left\{\sum_{\gamma'} \left[\left(\prod_{\gamma\in\Gamma,\gamma\neq\gamma'} -\mathcal{K}\bar{R}\gamma\right)(-\mathcal{K}\bar{R}\partial\gamma')\right] G/\Gamma + \left(\prod_{\gamma\in\Gamma} -\mathcal{K}\bar{R}\gamma\right)\partial(G/\Gamma)\right\}.$$

With Eq. (12A.1), this may be rewritten as

$$\begin{aligned}\partial\bar{R}G &= \sum_{\Gamma(G)} \left\{\sum_{\gamma'}\sum_{l\in\gamma'} \left[\left(\prod_{\gamma\in\Gamma,\gamma\neq\gamma'} -\mathcal{K}\bar{R}\gamma\right)(-\mathcal{K}\bar{R}\partial_l\gamma')\right] G/\Gamma \right. \\ &\qquad \left. + \sum_{l\in G/\Gamma} \left(\prod_{\gamma\in\Gamma} -\mathcal{K}\bar{R}\gamma\right)\partial_l G/\Gamma\right\}. \qquad (12A.2)\end{aligned}$$

The derivative ∂_l can be applied to those terms which do not contain lines l without any effect, leading to

$$\partial\bar{R}G = \sum_{\Gamma(G)} \left\{\sum_{l\in\Gamma} \left(\prod_{\gamma\in\Gamma} -(\mathcal{K}\bar{R}\partial_l\gamma)\right)\partial_l(G/\Gamma) + \sum_{l\in G/\Gamma} \left(\prod_{\gamma\in\Gamma} -\mathcal{K}\bar{R}\partial_l\gamma\right)\partial_l(G/\Gamma)\right\}.$$

Since each line l is either in Γ or in G/Γ, the two terms in the last equation can be combined to a single sum:

$$\partial\bar{R}G = \sum_{\Gamma(G)}\sum_{l\in G} \left(\prod_{\gamma\in\Gamma} -(\mathcal{K}\bar{R}\partial_l\gamma)\right)\partial_l(G/\Gamma). \qquad (12A.3)$$

The sum over the sets Γ can now be interchanged with the sum over l because the last one is independent of the choice of Γ. Hence

$$\partial\bar{R}G = \sum_{l\in G}\sum_{\Gamma(G)} \left(\prod_{\gamma\in\Gamma} -(\mathcal{K}\bar{R}\partial_l\gamma)\right)\partial_l(G/\Gamma). \qquad (12A.4)$$

To each set $\Gamma(G)$, there is a corresponding set $\Gamma(\partial G)$, and the sum can be rewritten as running over the sets $\Gamma(\partial G)$:

$$\partial\bar{R}G = \sum_{l\in G}\sum_{\Gamma(\partial G)} \left(\prod_{\gamma\in\Gamma} -(\mathcal{K}\bar{R}\gamma)\right)(\partial_l G/\Gamma). \qquad (12A.5)$$

The inner sum of this expression corresponds to the $\bar{R}$-operation of $\partial_l G$. Using the linearity of $\bar{R}$, the right-hand side can be brought to the desired form

$$\partial\bar{R}G = \sum_{l\in G} \bar{R}\partial_l G = \bar{R}\sum_{l\in G}\partial_l G = \bar{R}\partial G, \qquad (12A.6)$$

proving the interchangeability of differentiation and $\bar{R}$-Operation.

Notes and References

The citations in the text refer to:

[1] A.A. Vladimirov, Theor. Math. Phys. **36**, 732 (1978).

[2] K.G. Chetyrkin, F.V. Tkachov, Phys. Lett. B **114**, 240 (1982).

[3] K.G. Chetyrkin, V.A. Smirnov, Phys. Lett. B **144**, 419 (1984).

[4] D.R.T. Jones, Nucl. Phys. B **75**, 531 (1974).

[5] K.G. Chetyrkin, F.V. Tkachov, Nucl. Phys. B **192**, 159 (1981).

[6] The equivalent notation in the UV-case would be $(\gamma)_{UV} = \mathcal{K}\bar{R}(\gamma)$. But in the UV-case the implementation of the pole terms into the remaining diagram is much simpler, being always a product of $\mathcal{K}\bar{R}(\gamma)$ with the remaining diagram, and the result can be written down immediately. For this reason there was no advantage in introducing an ultraviolet object $(\gamma)_{UV}$.

[7] See also Appendix B of
W.E. Caswell, A.D. Kennedy, Phys. Rev. D **25**, 392 (1982).